AD_____

Award Number: W81XWH-13-1-0164

TITLE: Obesity Exposure Across the Lifespan on Ovarian Cancer Pathogenesis

PRINCIPAL INVESTIGATOR: Victoria Bae-Jump, M.D., Ph.D.

CONTRACTING ORGANIZATION:
The University of North Carolina at Chapel Hill
Chapel Hill, NC 27599-7295

REPORT DATE: June 2014

TYPE OF REPORT: Annual

PREPARED FOR: U.S. Army Medical Research and Materiel Command
Fort Detrick, Maryland 21702-5012

REPORT DOCUMENTATION PAGE

Form Approved
OMB No. 0704-0188

1. REPORT DATE 1 Jun 2014	**2. REPORT TYPE** Annual	**3. DATES COVERED** 01 June 2013 – 31 May 2014

4. TITLE AND SUBTITLE

Obesity Exposure Across the Lifespan on Ovarian Cancer Pathogenesis

5a. CONTRACT NUMBER

5b. GRANT NUMBER
W81XWH-13-1-0164

5c. PROGRAM ELEMENT NUMBER

6. AUTHOR(S)
Victoria Bae-Jump, M.D., Ph.D.
Betty Diamond

E-Mail: Victoria.Bae-Jump@unchealth.unc.edu

5d. PROJECT NUMBER

5e. TASK NUMBER

5f. WORK UNIT NUMBER

7. PERFORMING ORGANIZATION NAME(S) AND ADDRESS(ES) AND ADDRESS(ES)
The University of North Carolina at Chapel Hill
Lineberger Comprehensive Cancer Center
450 West Drive
CB 7295
Chapel Hill, NC 27599-2795

8. PERFORMING ORGANIZATION REPORT NUMBER

9. SPONSORING / MONITORING AGENCY NAME(S) AND ADDRESS(ES)
U.S. Army Medical Research and Materiel Command
Fort Detrick, Maryland 21702-5012

10. SPONSOR/MONITOR'S ACRONYM(S)

11. SPONSOR/MONITOR'S REPORT NUMBER(S)

12. DISTRIBUTION / AVAILABILITY STATEMENT
Approved for Public Release; Distribution Unlimited

13. SUPPLEMENTARY NOTES

14. ABSTRACT

Obesity is associated with increased risk and worse outcomes for ovarian cancer (OC). We theorize that the metabolic effects of obesity may play a contributing role in the pathogenesis of OC and lead to biologically different cancers than those that arise in normal weight women. We also posit that the timing and length of the obesity exposure may be critical in the development of obesity-driven OCs. We have demonstrated that adulthood exposure to obesity can promote tumor progression, as evidenced by a tripling in tumor size, in the KpB mouse model of serous OC. The ovarian tumors that arose in the obese mice were genomically and metabolically different from those that arose in non-obese mice. To expand on this work, we assessed in utero, adolescent and adulthood exposure to obesity as well as cross-over between these timeframes in the KpB mice. Longer exposure to obesity resulted in greater tumor weight and shorter tumor latency, especially in diet exposures that included in utero exposure to obesity. Using The Cancer Genome Atlas database, we compared the gene expression between OCs from normal weight versus overweight/obese women. Metabolically relevant alterations in gene expression were found in relationship to BMI status among serous OCs.

15. SUBJECT TERMS
ovarian cancer, obesity, mTOR pathway, mouse model, metabolomics, genomics, The Cancer Genome Atlas Project

16. SECURITY CLASSIFICATION OF:			**17. LIMITATION OF ABSTRACT**	**18. NUMBER OF PAGES**	**19a. NAME OF RESPONSIBLE PERSON** USAMRMC
a. REPORT U	**b. ABSTRACT** U	**c. THIS PAGE** U	UU	37	**19b. TELEPHONE NUMBER** *(include area code)*

Table of Contents

INTRODUCTION

Epithelial ovarian cancer is one of the most deadly cancers with an overall 5-year survival of only 30-40%. Increasing evidence suggests that obesity is a significant risk factor for ovarian cancer and is associated with worse outcomes for this disease (1-14). Less is known of the impact of the timing of the obesity exposure, but some epidemiological studies suggest that adolescent exposure to obesity bears the greatest increased risk for ovarian cancer development (12, 15). We hypothesize that the metabolic and endocrine effects of obesity play a role in the carcinogenesis of ovarian cancer and invariably lead to biologically distinct cancers than those that arise in leaner women, possibly through aberrant modulation of mTOR signaling in an obesity-specific mechanism. An understanding of the relationship between obesity across the lifespan of a woman, and mTOR activation in ovarian cancer pathogenesis has yet to be explored and makes this proposal novel. This translational proposal will address this gap in knowledge by investigating the impact of the timing of the obesity exposure *in vivo* and *in vitro* using a novel serous ovarian tumor murine model and in ovarian cancer tumors from obese and non-obese women via interrogation of The Cancer Genome Atlas (TCGA) Project database. We postulate that *in utero* and adolescent exposure to obesity will increase vulnerability to ovarian cancer, and this will be manifested in obesity-specific mTOR hyperactivation and its downstream effects on enhanced proliferation and an advantageous metabolic profile.

BODY

Task 1 (Aim 1): To compare tumor latency and growth in K18-gT$_{121}^{+/-}$;p53$^{fl/fl}$;Brca1$^{fl/fl}$ (KpB) mice exposed to a high fat diet at different time points across the lifespan, including *in utero*, adolescence and adulthood.

We have previously described a unique serous ovarian cancer mouse model that specifically and somatically deletes the tumor suppressor genes, Brca1 and p53, and inactivates the retinoblastoma (Rb) proteins in adult ovarian surface epithelial cells (KpB mouse model) (45, 46). Subsequently, KpB mice were subjected to a 60% calories-derived from fat in a high fat diet (HFD) *versus* 10% calories from fat in a low fat diet (LFD) to induce diet-induced obesity (N=14/group) starting at 6 weeks of age and until sacrifice. After 8 months of exposure to the HFD or LFD, obese mice weighed significantly greater than non-obese mice (p=0.003, Table 1). There was no effect of HFD on non-fasted blood glucose levels or diabetes onset in KpB mice over the course of the diet (Table 1). Body composition was significantly altered in obese KpB mice compared to non-obese controls. Percent body fat was six-fold greater in obese mice (Table 1, p=0.0001), while percent lean mass increased by 25% (p=0.0006, Table 1). The ovarian tumors were tripled in size in the obese mice as compared to non-obese mice (mean size of 3.7 cm^2 *versus* 1.2 cm^2, **Figure 1**, p=0.0065). This suggests that obesity can promote tumor progression in the KpB mouse model of ovarian cancer.

Table 1. Diet-induced metabolic characteristics in non-obese and obese KpB mice.

	Non-Obese	Obese	p-value
Weight (gms)	31.14 ± 5.26	50.71 ± 16.73	p=0.0003
Glucose (mg/dl)	186.81 ± 26.99	214.38 ± 58.11	p=0.053
% Fat	3.28 ± 1.51	19.58 ± 7.88	p=0.00001
% Lean	22.89 ± 2.11	28.66 ± 5.24	p=0.0006

N=14 mice per group. Mean ± SD. % Fat or % lean = each mass/total body mass as measured by MRI.

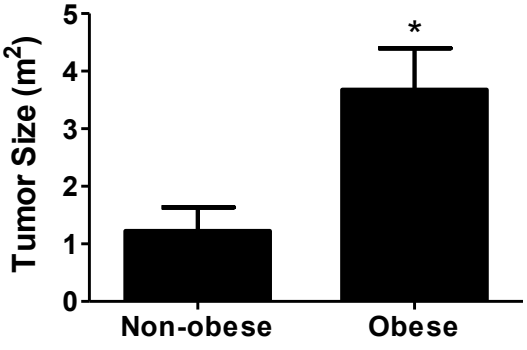

Figure 1. Obesity increases tumor size in KpB mice. KpB mice were fed low fat or high fat diets to induce obesity for 6 months during tumorigenesis. (A) Comparison of tumor size from non-obese and obese mice (N=14). These mice were sacrificed 6 months after ovarian tumor induction via injection of AdCre into the ovarian bursa cavity. For the calculation of tumor size, the greatest longitudinal diameter (length) and the greatest transverse diameter (width) were determined and multiplied (m^2). *p=0.0065.

Obesity was found to induce genomic differences between the obese and non-obese ovarian tumors. 439 genes were found to be significantly up-regulated (417 genes) or down-regulated (22 genes) in the ovarian tumors from obese KpB mice *versus* non-obese mice (FDR<0.2). **Figure 2** is a heat map of 131 genes up- and down-regulated at a FDR<0.1. Many metabolically relevant genes were significantly upregulated in the ovarian tumors from the obese *versus* non-obese mice, such as lipocalin (2.7 fold), fatty acid amide hydrolase (2.7 fold), fatty acid 2-hydroxylase (2.2 fold), glycerol-3-phosphate acyltransferase (1.5 fold), protein phosphatase (1.2 fold), AMP deaminase 3 (1.6 fold), and protein kinase C (1.7 fold). Arginase 1 was the most upregulated gene (7.3 fold) and plays a role in the urea cycle, tissue remodeling and inflammation. Other upregulated genes identified in the ovarian tumors from the obese mice were related to cell adhesion, including neurotrimin (2.2 fold) and desmoglein 1-alpha (2.0 fold). Increased expression of histone 1 (2.3 fold) and endothelin-1 (5.8 fold) were also associated with obesity in the KpB mouse model. Another gene upregulated 3 fold was ectonucleoside triphosphate diphosphohydrolase. Heparan sulfate (glucosamine) 3-O-sulfotransferase 1 was upregulated 6 fold and regulates heparan sulfate production which is involved in developmental processes, angiogenesis, blood coagulation and tumor metastasis. The serotonin transporter solute carrier family 6 member 4 (Slc6a4) was upregulated 5.4 fold by obesity. Important downregulated genes included spermidine synthase, an enzyme in spermidine synthesis and thrombospondin 4, an extracellular glycoprotein known to have roles in cellular migration, adhesion, attachment and proliferation. In the ovarian tumors from the obese *versus* non-obese mice, DAVID functional annotation analysis revealed significant enrichment in “phospoholipid binding” (EASE score of 0.008), “regulation of apoptosis” (EASE score of 0.014), “lipid binding” (EASE score of 0.015), “endopeptidase activity” (EASE score of 0.03) and “cell-cell signaling” (EASE score of 0.44) for those identified genes.

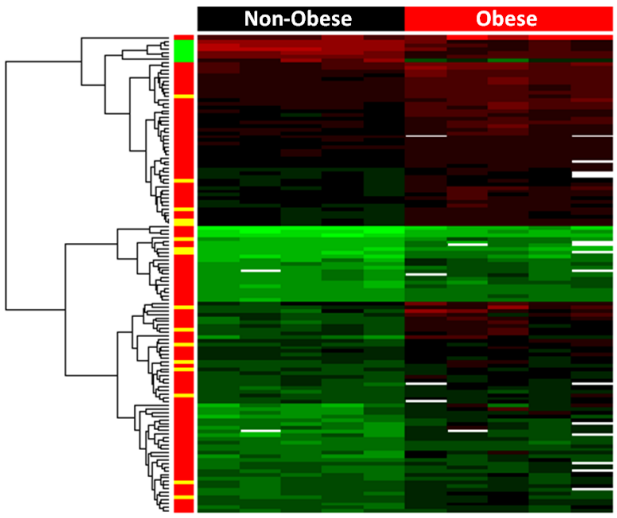

Figure 2. Genomic differences between ovarian tumors from obese *versus* non-obese KpB mice reveal alterations in metabolically relevant genes. Heat map representation of 131 genes significantly up- or down-regulated in ovarian tumors from obese *versus* non-obese KpB mice (FDR<0.1). Many metabolically relevant genes, such as lipocalin, fatty acid amide hydrolase, ectonucleoside triphosphate diphosphohydrolase, fatty acid 2-hydroxylase, glycerol-3-phosphate acyltransferase, protein phosphatase, protein kinase C and AMP deaminase 3, were upregulated in obese tumors.

Metabolic differences were also found between the ovarian tumors from obese and non-obese KpB mice. Principle component analysis defined a clear separation between obese and non-obese. Differentiating metabolites were selected with the criteria of the variable importance in the projection (VIP) value>1 and *p* value (Student’s *t* test) lower than 0.05. Twenty metabolites were identified using this criteria, all of which were upregulated in the ovarian tumors of the non-obese *versus* obese KpB mice (Table 2).

Metabolites involved in inflammatory signaling and protein/collagen metabolism were down-regulated in the ovarian tumors of obese mice as compared to non-obese mice, including arginine (p=0.0268), N-glycylproline (p=0.0043) and 3-amino-2-piperidone (p=0.0099). Components and markers of oxidative stress were also downregulated in the tumors from obese mice: glutathione (p=0.0313), oxidized glutathione (p=0.0047), gluconolactone (p=0.0311) and 8-hydroxy-deoxyguanosine (p=0.0230). Lower levels of nucelotides (i.e. cytidine (p=0.0122 and p=0.0424), cytosine (p=0.0158), guanosine diphosphate (GDP, p=0.0404)) and adenosine monophosphate (AMP, p=0.0257) were detected with obesity. The serotonin metabolite, 5-hydroxyindoleacetic acid (5HIAA, p=0.0498), and the catecholamine metabolites, vanillactic acid (p=0.0079) and phenylethanolamine (p=0.0446), were found to be lower in the ovarian tumors of obese *versus* non-obese mice. Glutamate (p=.0318), N-acetylaspartic acid (p=0.0059) and succinic acid (p=0.0465) are involved in energy metabolism, and were decreased in the ovarian tumors of obese KpB mice as compared to their non-obese counterparts. LysoPC(16:1(9Z)) (p=0.0205), a lysophospholipid, and the metabolite of a toxic intermediate, inodxyl glucuronide (p=0.0439), were also lower in the ovarian tumors from obese animals.

Table 2. Metabolic alterations in tumors from non-obese and obese KpB mice.

Compound name	VIP [a]	*p* [b]	Fold Change (non-obese/obese) [c]	Analysis method	Identification Method [e]
N-Glycylproline	2.27	0.0043	1.95	LC-ES+	Std
Oxidized glutathione	2.25	0.0047	3.45	LC-ES+	Std
N-Acetylaspartic acid	2.22	0.0059	2.31	LC-ES-	HMDB
Vanillactic acid	2.17	0.0079	2.23	LC-ES+	HMDB
3-amino-2-piperidone	2.14	0.0099	1.75	GCTOF	NIST
Cytidine	2.10	0.0122	4.52	LC-ES+	Std
Cytosine	2.05	0.0158	4.11	LC-ES+	Std
LysoPC(16:1(9Z))	1.99	0.0205	1.83	LC-ES+	HMDB
8-Hydroxy-deoxyguanosine	1.97	0.0230	2.45	LC-ES+	HMDB
Adenosine monophosphate	1.94	0.0257	1.61	LC-ES-	HMDB
Arginine	1.93	0.0268	1.93	LC-ES+	Std
Gluconolactone	1.89	0.0311	2.97	LC-ES+	Std
Glutathione	1.89	0.0313	3.10	LC-ES+	Std
Glutamate	1.89	0.0318	1.52	GCTOF	Std
Guanosine diphosphate	1.82	0.0404	2.39	LC-ES-	HMDB
Cytidine	1.81	0.0424	4.97	GCTOF	NIST
Inodxyl glucuronide	1.80	0.0439	3.05	LC-ES+	HMDB
Phenylethanolamine	1.80	0.0446	1.69	GCTOF	NIST
Succinic acid	1.78	0.0465	1.90	GCTOF	Std
5-Hydroxyindoleacetic acid	1.76	0.0498	1.85	LC-ES+	HMDB

[a] variable importance in the projection (VIP) was obtained from OPLS-DA with a threshold of 1.0; [b] *p* value was calculated from Student's *t* Test; [c] Fold change with a value larger than 1 indicates a relatively higher concentration in tumors from non-obese (low fat diet-fed) KpB mice, while a value less than 1 means a relatively lower concentration as compared to tumors from obese (high fat diet-fed) KpB mice. [e] The metabolites were identified by in-house library (Std), NIST library (NIST) or HMBD database (HMDB).

To further expand on this work, the KpB ovarian cancer mouse model was used to assess the tumor promoting effect of high fat diet (HFD)-diet-induced obesity on tumor initiation and promotion amongst different *obesity exposures across the lifespan*. KpB mice were placed on a LFD or a HFD at different time points during their lifespan, including *in utero*, adolescence and adulthood. Cross-over diet study design was employed to examine if weight loss by switching from a HFD to a LFD reverses elevated risk associated

Table 3. Diet Study using the KpB ovarian cancer mouse model to identify relevant windows of susceptibility to obesity-induced risk. The effect of obesity on tumor promotion in mice made obese by high fat diet versus non-obese mice at relevant periods of vulnerability including *in utero*, adolescence and adulthood as well as combinations of these exposures were explored.

Group	*In utero* exposure	Adolescent exposure	Adulthood exposure
A	LFD	LFD	LFD
B	LFD	LFD	HFD
C	LFD	HFD	HFD
D	LFD	HFD	LFD
E	HFD	HFD	HFD
F	HFD	HFD	LFD
G	HFD	LFD	LFD
H	HFD	LFD	HFD

with obesity. Eight different diet exposures were examined, as depicted in **Table 3**.

Tumor weight (grams) was found to be larger when comparing group A (no exposure to a HFD; LFD *in utero* + adolescence + adulthood) to groups E (HFD *in utero* + adolescence + adulthood), F (HFD *in utero* + HFD in adolescence + LFD in adulthood) and H (HFD *in utero* + LFD in adolescence + HFD in adulthood) (**Figure 3A**). Tumor latency was found to be shorter when comparing group A (no exposure to a HFD; LFD *in utero* + adolescence + adulthood) to groups F (HFD *in utero* + HFD in adolescence + LFD in adulthood) and H (HFD *in utero* + LFD in adolescence + HFD in adulthood) (**Figure 3B**). Common to all the groups that had a statistically significant difference in either tumor weight or tumor latency compared to group A (no exposure to a HFD) was (1) *in utero* exposure to a HFD and (2) exposure to a HFD for at least two different timeframes across the lifespan of the mouse. This data is based on 6-8 mice per group; however, all of the data is not complete with an expected 12-15 mice per group at the completion of the study. **This preliminary data does suggest that longer exposure to a HFD results in greater tumor weight and shorter tumor latency.**

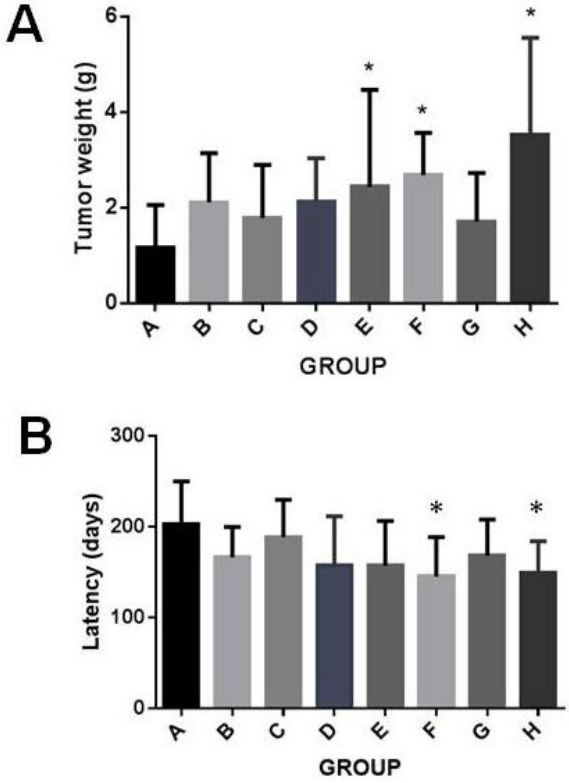

Figure 3. Obesity increases tumor weight (A) and latency (B) in KpB mice. KpB mice were placed on a LFD or a HFD at different time points during their lifespan, including *in utero*, adolescence and adulthood. (see **Table 3** for description of groups) (*p<0.05)

The weight of the mice was also greater in the groups with longer exposure to the HFD. When compared to group A (LFD *in utero* + adolescence + adulthood), groups B (LFD *in utero* + LFD in adolescence + HFD in adulthood), C (LFD *in utero* + HFD in adolescence + HFD in adulthood), E (HFD *in utero* + HFD in adolescence + HFD in adulthood) and H (HFD *in utero* + LFD in adolescence + HFD in adulthood) (**Figure 4**). Common to all the groups that had a statistically significant difference in mouse weight compared to group A (no exposure to a HFD) was adulthood exposure to a HFD. There were no significant changes in blood glucose levels among the eight groups (data not shown). The ovarian tumors from each of these groups has been frozen for gene expression profiling and metabolomic comparative analysis in the upcoming year.

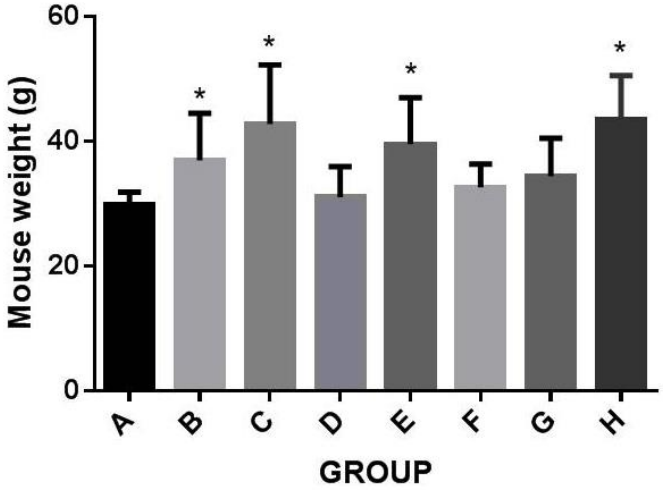

Figure 4. Exposure to a HFD increases the weight of the KpB mice. KpB mice were placed on a LFD or a HFD at different time points during their lifespan, including *in utero*, adolescence and adulthood. (see **Table 3** for description of groups) (*p<0.05)

Task 2 (Aim 2): To determine if PI3K/Akt/mTOR pathway hyperactivation and alterations in glucose metabolism are related to obesity-driven cancers in the KpB ovarian cancer mouse model.

We are waiting to sacrifice the rest of the KpB mice in each of the diet groups before we can proceed with this aim. As part of this aim, ovarian tumors from the KpB mice that were exposed to obesity initiated *in utero versus* adolescence *versus* adulthood *versus* combinations of these exposures will undergo Western immunoblotting and immunohistochemical analysis to assess for

differences in the phosphorylated and/or total forms of the downstream target proteins of the IGF-1R and PI3K/Akt/mTOR pathway. A subset of these ovarian cancer tumors will be used for primary culture to assess for secretion of growth factors associated with ovarian carcinogenesis (i.e. IGF-1) and perturbations in glucose metabolism as evaluated by ELISA and metabolic assays, respectively.

Task 3 (Aim 3): To assess cross-species differences of the gene expression profiles of ovarian cancer tumors from obese and non-obese women and KpB mice, using the relevant tumor data from The Cancer Genome Atlas (TCGA) Project database.

From the TCGA database, we collected expression measurements for 12,042 genes from the platform (BI_HT_HG-U133A level 3 data) for differential gene expression analysis among human serous OC samples. The detailed information of the data processing, quality control and normalization can be found on the TCGA website. To identify significantly differentially expressed genes associated with BMI, we applied linear modeling for responses as gene expression and covariates as 5 principal components (PCs) (from gene expression data to control potential batch effects), clinical stage, grade, age, race, residual tumor and BMI status (0 if normal BMI < 25; 1 if overweight BMI ≥ 25). Appropriate false discovery rates (FDR) were controlled. With the obtained genes that were significantly associated with BMI status, we conducted functional clustering analysis on the website of The Database for Annotation, Visualization and Integrated Discovery (DAVID). In addition, we applied hierarchical clustering analysis to generate a representative heatmap. The Chi-square test was used to compare BMI among different clusters of samples. A comparison of the demographics between the ovarian cancer tumors from normal weight (BM I< 25) and overweight/obese women (BMI ≥ 25) can be found in **Table 4**.

Table 4. Comparison of the demographics between the ovarian cancer tumors from normal weight and overweight/obese women.

	BMI < 25 (Normal Weight) (N=99)	**BMI ≥ 25 (Overweight/Obese) (N=138)**
Age (mean)	57.9	59.4
Race		
White	89 (90%)	125 (91%)
Black	5 (5%)	11 (8%)
Other	5 (5%)	2 (1%)
Grade		
2	11 (11%)	12 (9%)
3	88 (89%)	126 (91%)
Stage		
I/II	2 (2%)	4 (3%)
III/IV	97 (98%)	134 (97%)
Residual Disease		
Optimal	75 (76%)	99 (72%)
Suboptimal	24 (24%)	39 (28%)

347 genes were found to be significantly up- or down-regulated with BMI status (BMI < 25 *versus* BMI ≥ 25) among the serous ovarian tumors (q-value < 0.1), including metabolically relevant genes (**Supplemental Tables 1 and 2**). Genes that were down-regulated included the prolactin receptor (3.6 fold) and apolipoprotein B mRNA editing enzyme (3.1 fold), among others. Genes that were up-regulated included mitogen-activated protein kinase 1 (3.3 fold), phospholipid scramblase 1 (3.3 fold), carnitine/acylcarnitine translocase (3.2 fold), low density lipoprotein receptor-related protein 8 (apolipoprotein e receptor) (3.7 fold), apolipoprotein L3 (3.7 fold), apolipoprotein L1 (3.8 fold), lipoyltransferase 1 (4.2 fold), apolipoprotein L6 (4.2 fold) and the c-myc binding protein (4.1 fold). Many of these genes were related to the apolipoprotein pathway, particularly apolipoprotein L related genes. Apolipoprotein L genes are members of the high density lipoprotein family and play a central role in cholesterol transport. Multiple genes involving the Ras oncogene family were up- and down-regulated when comparing normal weight versus overweight/obese women, including ras responsive element binding protein 1, RAB5C, RREB1, ras-related GTP binding C, PAP1A, RAB7A, RAB31, RAB5A, and ras homolog family/member A. DAVID functional annotation analysis revealed significant enrichment in "protein transport" (Adjusted p-value for Benjamini = 5.5E-5), "antigen processing and presentation of exogenous peptide antigen" (Adjusted p-value for Benjamini = 1.3E-3) and "pyrimidine ribonucleotide biosynthetic process" (Adjusted p-value for Benjamini = 3.6E-2) for these identified genes.

Initially, we used the 347 genes with q-value < 0.1 to generate a heatmap, but the results of the hierarchical cluster analysis on these samples did not group them with a significantly different BMI distribution. Alternatively, we used the 175 genes with q-value < 0.05 to generate a heatmap, which is presented in **Figure 5**, where the row signifies gene expression and the column is clustering according to BMI (BMI < 25 *versus* BMI ≥ 25). If we specified two groups to cut a tree resulting from the results of the hierarchical cluster analysis on the samples, the two clusters of samples had no statistically significant difference in the distribution of BMI. However, if we specified three groups to cut a tree resulting from the results of the hierarchical cluster analysis, there were two pairs of clusters of samples with a significantly different distribution of BMI. Specifically, the first pair of clusters of samples (cluster 1 *versus* cluster 2) had sample proportions of subjects with BMI ≥ 25 (0.65, 0.33). For testing if the two proportions are significantly different, the obtained Chi-square statistics was 7.87, df = 1 and p-value = 0.005, suggesting that the two sample proportions are significantly different. The second pair of clusters of samples (cluster 3 *versus* cluster 2) had sample proportions of subjects with BMI ≥ 25 (0.61, 0.33). For testing if the two proportions are significantly different, the obtained Chi-square statistics was 11.36, df = 1 and p-value = 0.00075, suggesting that the two sample proportions are significantly different. In addition, there was significant difference in the proportions of women with a BMI ≥ 25 for cluster 1 and cluster 3 (0.65, 0.61). In summary, the analysis of the 175 gene set resulted in three sample clusters, with statistically significant differences in proportions of women with BMI ≥ 25 *versus* BMI <25 among these clusters. A summary of the genes in gene cluster 1 and 2 can be found in **Table 5**.

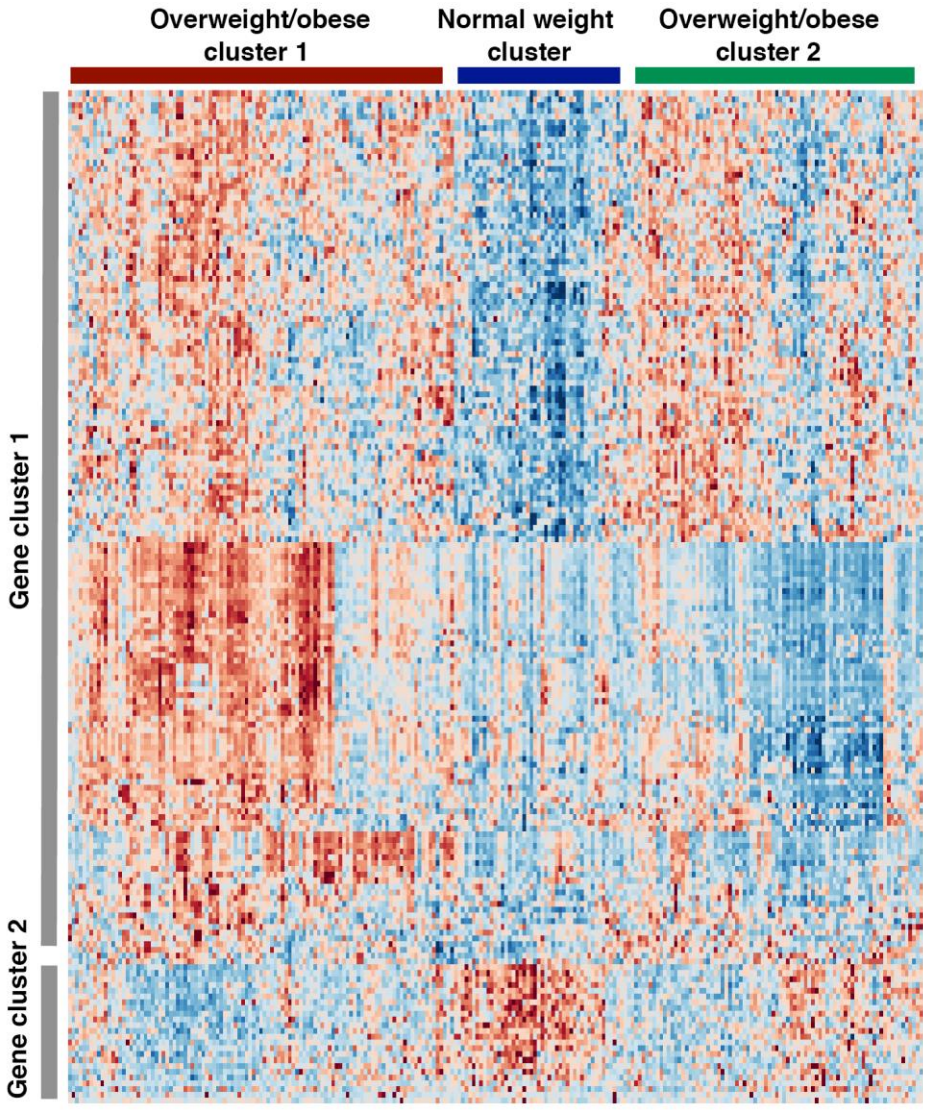

Figure 5. Genomic differences between ovarian tumors from normal weight *versus* overweight/obese women reveal alterations in metabolically relevant genes. Heat map representation of 264 genes significantly up- or down-regulated in ovarian tumors from normal weight *versus* overweight/obese women (FDR<0.05). Many metabolically relevant genes were upregulated in ovarian tumors from overweight/obese women such as mitogen-activated protein kinase 1, phospholipid scramblase 1, carnitine/acylcarnitine translocase, low density lipoprotein receptor-related protein 8 (apolipoprotein e receptor), apolipoprotein L3, apolipoprotein L1, lipoyltransferase 1, apolipoprotein L6 and the c-myc binding protein.

KEY RESEARCH ACCOMPLISHMENTS

- The obese state can promote tumor progression in the KpB mouse model of ovarian cancer. Longer exposures to obesity had the greatest impact on tumor weight.
- Distinct metabolic and genomic differences were identified in ovarian

tumors that arose in KpB mice after adulthood exposure to a HFD *versus* a LFD, and many of these differences were related to metabolic relevant pathways.

- Metabolically relevant alterations in gene expression were found with increasing BMI among human serous ovarian cancers, using the TCGA database.

Table 5. Gene Clusters of the Ovarian Tumors from Normal Weight (BMI<25) and Overweight/Obese Women (BMI≥25).

	Gene Name	David Gene Name
Gene Cluster 1	FAP	fibroblast activation protein, alpha
	LAIR1	leukocyte-associated immunoglobulin-like receptor 1
	GPR65	G protein-coupled receptor 65
	RAB5C	RAB5C, member RAS oncogene family
	CTSK	cathepsin K
	RHOA	Ras homolog gene family, member A
	RAB5A	RAB5A, memver RAS oncogene family
	IL10RA	interleukin 10 recptor, alpha
	IL2RB	interluekin 2 receptor, beta
	LRP8	low density lipoprotein receptor-related protein 8
	APOL3	apolipoprotein L3
	APOL1	apolipoprotein L1
	CFLAR	CASP8 and FADD-like apoptosis regulator
	PLAU	plasminogen activator, urokinase
	RAB31	RAB31, member RAS oncogene family
	MYCBP	c-myc binding protein
	AAPOL6	apolipoprotein L6
	LIPT1	lipoyltransferase 1
	PRKAA1	protein kinase, AMP-activated, alpha 1 catalytic subunit
	PTPRC	protein tyrosine phosphotase, receptor type, C
	ETF1	eukaryotic translation termination factor 1
	EIF2B3	eukaryotic translational initiation factor 2B
	CASP1	caspase 1, apoptosis-related cysteine peptidase
Gene Cluster 2	IGSF3	immunoglobulin superfamily, member 3
	PRLR	prolactin receptor
	GRM4	glutamate receptor, metabotropic 4
	LY6G6E	lymphocyte antigen 6 complex, locus G6E
	GRIN1	glutamate receptor, ionotropic, N-methyl D-aspartate 1
	ADRA1A	adrenergic, alpha-1A-, receptor

REPORTABLE OUTCOMES

Abstracts presented:
(1) Zhou, C, Zhong, Y, Du, X, Makowski, L, Jia, W and Bae-Jump, VL, Diet-induced obesity increases tumor aggressiveness in a genetically engineered mouse model of serous ovarian cancer, Oral Presentation by Dr. Bae-Jump at the 2013 Annual Meeting of the Society of Gynecologic Oncology.

Manuscripts accepted:
(1) Makowski, L, Zhou, C, Zhong, Y, Kuan, PF, Fan, Sampey, BP, Difurio, M and Bae-Jump, VL. Obesity increases tumor aggressiveness in a genetically engineered mouse model of serous ovarian cancer. Gynecologic Oncology, 133(1):90-7 (2014). PMID: 24680597

Grants submitted:
(1) 1R01 - AN:3701643
Obesity, Cation-Selective Transporters and Metformin in Endometrial Cancer
Co-Principal Investigator: Bae-Jump
15% effort (1.8 calendar)
Mounting epidemiological and preclinical data suggest that metformin may be efficacious in endometrial cancer. However, two important questions that need to be addressed are: **(1)** Will metformin be universally effective in endometrial cancer or be more efficacious in the obese/insulin-resistant patient population? and **(2)** What role do transporters play in metformin uptake and action in the malignant endometrium? These fundamental questions will be explored in endometrial cancer, a disease driven by obesity and insulin resistance, using endometrial cancer mouse models and phase 0 and phase 2/3 clinical trials in endometrial cancer patients.

(2) American Cancer Society/Research Scholar Grant
Obesity, Cation-Selective Transporters and Metformin in Endometrial Cancer
Co-Principal Investigator: Bae-Jump
10% effort (1.2 calendar)
Mounting epidemiological and preclinical data suggest that metformin may be efficacious in endometrial cancer. However, two important questions that need to be addressed are: **(1)** Will metformin be universally effective in endometrial cancer or be more efficacious in the obese/insulin-resistant patient population? and **(2)** What role do transporters play in metformin uptake and action in the malignant endometrium? These fundamental questions will be explored in endometrial cancer, a disease driven by obesity and insulin resistance, using endometrial cancer mouse models and phase 0 and phase 2/3 clinical trials in endometrial cancer patients.

CONCLUSION

Obesity is associated with increased risk and worse outcomes for OC, and alterations in PI3K/Akt/mTOR signaling may play a crucial role in this relationship with potential implications for prevention and improvement of outcomes for this disease. We and others have made significant progress investigating the effects of obesity on tumor cell growth, but an understanding of the interactions between obesity at specific vulnerable periods of development, OC and the PI3K/Akt/mTOR pathway is lacking. We theorize that the metabolic effects of obesity play a contributing role in the pathogenesis of OC and lead to phenotypically different cancers than those that arise in leaner women, potentially through hyperactivation of the mTOR kinase. We also posit that the timing and length of the obesity exposure is critical in the development of obesity-driven OCs. Although the PI3K/Akt/mTOR pathway is known to be separately important in obesity and OC, the complex interplay between both of these disease entities on PI3k/Akt/mTOR signaling in OC has not been simultaneously assessed. Our multi-dimensional approach is innovative because utilizes several tools including a unique genetically engineered mouse model (GEMM), cell lines and patient samples to comprehensively interrogate the obesity-induced carcinogenesis signature through molecular, biochemical, genomic and metabolomic analysis. While the PI3K/AKT/mTOR pathway is a likely candidate pathway, the

defined approach will identify additional genes and metabolites heretofore underappreciated in OC that are dependent upon windows of obesity exposure.

To first study the connection between metabolic status and OC, we capitalized upon the novel K18-$gT_{121}^{+/-}$;$p53^{fl/fl}$;$Brca1^{fl/fl}$ (KpB) OC genetically engineered mouse model (GEMM) in the obesity-susceptible FVB/N background. KpB mice were used to investigate the impact of obesity on OC pathogenesis and to test the effects of varying the timing and length of the obesity exposure across the lifespan, including *in utero*, adolescence and adulthood. Adulthood exposure to obesity in the KpB mouse model accelerated tumorigenesis. A tripling of tumor mass was found in KpB mice fed a high fat obesogenic diet *versus* a low fat control diet in our initial pilot study. Gene expression and metabolomic profiling indicated statistically significant differences between the ovarian tumors from the obese *versus* non-obese mice, including metabolically relevant pathways.

We expanded on this work to assess which windows of exposure to obesity are most important for increased vulnerability and progression of OC. Eight different diet exposures were examined, as depicted in **Table 3**. Longer exposure to a HFD resulted in greater tumor weight and shorter tumor latency, especially in diet exposures that included *in utero* exposure to obesity. The weight of the mice was also greater in the groups with longer exposure to a HFD, particularly those mice with adulthood exposure to a HFD. The ovarian tumors from each of these eight groups has been frozen for gene expression profiling and metabolomic comparative analysis as well as western blotting and immunohistochemical analysis for downstream targets of the PI3K/Akt/mTOR pathway. In the upcoming year, ovarian tumors from obese and non-obese mice will also be examined in primary culture as a means to interrogate the effects of the obesity exposure on mTOR hyperactivation and glucose metabolism, or pathways identified through genomics and metabolomics.

This proposal aims next to translate *in vitro* and preclinical studies into human relevance and explore the impact of obesity on human OC. Using The Cancer Genome Atlas (TCGA) database, we compared the gene expression between OCs from normal weight *versus* overweight/obese women. Metabolically relevant alterations in gene expression were found in relationship to BMI status among serous OCs, including multiple genes related to the apolipoprotein pathway. Apolipoproteins are proteins that bind lipids (oil-soluble substances such as fat and cholesterol) to form lipoproteins for transport through the lymphatic and circulatory systems. This will be pathway of interest for our future studies. In the upcoming year, cross-species gene expression comparisons of OC tumors derived from obese and non-obese women and KpB mice will be used as a strategy to identify obesity-dependent biomarkers and potential novel targets of treatment. Cross-species comparisons will lend strength to findings from either strategy, thus creating a powerful experimental paradigm. The proposed study design is innovative because the tools we will use such as the KpB mouse model and the TCGA database allows us to focus on the tumor/host interaction, especially in regards to obesity-driven effects. Through these complementary studies, we will advance the understanding of OC's metabolic and genomic responses to the tumor promoting environment of obesity and determine the impact of the timing and length of the obesity exposure on ovarian carcinogenesis.

REFERENCES

1. Delort L, Kwiatkowski F, Chalabi N, Satih S, Bignon YJ, Bernard-Gallon DJ. Central adiposity as a major risk factor of ovarian cancer. Anticancer Res. 2009;29(12):5229-34. PubMed PMID: 20044641.
2. Pavelka JC, Brown RS, Karlan BY, Cass I, Leuchter RS, Lagasse LD, et al. Effect of obesity on survival in epithelial ovarian cancer. Cancer. 2006;107(7):1520-4. PubMed PMID: 16941453.
3. Olsen CM, Green AC, Whiteman DC, Sadeghi S, Kolahdooz F, Webb PM. Obesity and the risk of epithelial ovarian cancer: a systematic review and meta-analysis. Eur J Cancer. 2007;43(4):690-709. PubMed PMID: 17223544.
4. Leitzmann MF, Koebnick C, Danforth KN, Brinton LA, Moore SC, Hollenbeck AR, et al. Body mass index and risk of ovarian cancer. Cancer. 2009;115(4):812-22. PubMed PMID: 19127552.
5. Guh DP, Zhang W, Bansback N, Amarsi Z, Birmingham CL, Anis AH. The incidence of co-morbidities related to obesity and overweight: a systematic review and meta-analysis. BMC Public Health. 2009;9:88. PubMed PMID: 19320986.
6. Lahmann PH, Cust AE, Friedenreich CM, Schulz M, Lukanova A, Kaaks R, et al. Anthropometric measures and epithelial ovarian cancer risk in the European Prospective Investigation into Cancer and Nutrition. Int J Cancer.126(10):2404-15. PubMed PMID: 19821492.

7. Calle EE, Rodriguez C, Walker-Thurmond K, Thun MJ. Overweight, obesity, and mortality from cancer in a prospectively studied cohort of U.S. adults. The New England journal of medicine. 2003;348(17):1625-38. PubMed PMID: 12711737.
8. Schouten LJ, Goldbohm RA, van den Brandt PA. Height, weight, weight change, and ovarian cancer risk in the Netherlands cohort study on diet and cancer. Am J Epidemiol. 2003;157(5):424-33. Epub 2003/03/05. PubMed PMID: 12615607.
9. Fairfield KM, Willett WC, Rosner BA, Manson JE, Speizer FE, Hankinson SE. Obesity, weight gain, and ovarian cancer. Obstet Gynecol. 2002;100(2):288-96. Epub 2002/08/02. PubMed PMID: 12151152.
10. Chionh F, Baglietto L, Krishnan K, English DR, MacInnis RJ, Gertig DM, et al. Physical activity, body size and composition, and risk of ovarian cancer. Cancer causes & control : CCC. 2010;21(12):2183-94. Epub 2010/09/10. doi: 10.1007/s10552-010-9638-y. PubMed PMID: 20827504.
11. Rodriguez C, Calle EE, Fakhrabadi-Shokoohi D, Jacobs EJ, Thun MJ. Body mass index, height, and the risk of ovarian cancer mortality in a prospective cohort of postmenopausal women. Cancer Epidemiol Biomarkers Prev. 2002;11(9):822-8. Epub 2002/09/12. PubMed PMID: 12223425.
12. Lubin F, Chetrit A, Freedman LS, Alfandary E, Fishler Y, Nitzan H, et al. Body mass index at age 18 years and during adult life and ovarian cancer risk. American journal of epidemiology. 2003;157(2):113-20. Epub 2003/01/11. PubMed PMID: 12522018.
13. Engeland A, Tretli S, Bjorge T. Height, body mass index, and ovarian cancer: a follow-up of 1.1 million Norwegian women. J Natl Cancer Inst. 2003;95(16):1244-8. Epub 2003/08/21. PubMed PMID: 12928351.
14. Reeves GK, Pirie K, Beral V, Green J, Spencer E, Bull D. Cancer incidence and mortality in relation to body mass index in the Million Women Study: cohort study. BMJ. 2007;335(7630):1134. Epub 2007/11/08. doi: 10.1136/bmj.39367.495995.AE. PubMed PMID: 17986716; PubMed Central PMCID: PMC2099519.
15. Engeland A, Bjorge T, Selmer RM, Tverdal A. Height and body mass index in relation to total mortality. Epidemiology. 2003;14(3):293-9. Epub 2003/07/16. PubMed PMID: 12859029.

Supplemental Table 1. Genes Down-regulated when Comparing Ovarian Tumors from Normal Weight (BMI < 25) versus Overweight/Obese (BMI ≥ 25) Women.

Gene Name	David Gene Name	beta	pval	qval
TRIM31	tripartite motif-containing 31	-4.48216	1.18E-05	0.010901
ADCY2	adenylate cyclase 2 (brain)	-4.38132	1.81E-05	0.012207
NPPC	natriuretic peptide precursor C	-4.14758	4.76E-05	0.017198
ST8SIA2	ST8 alpha-N-acetyl-neuraminide alpha-2,8-sialyltransferase 2	-4.10055	5.76E-05	0.017198
PRRG3	proline rich Gla (G-carboxyglutamic acid) 3 (transmembrane)	-4.04219	7.27E-05	0.018246
AFF3	AF4/FMR2 family, member 3	-4.01323	8.16E-05	0.019262
LRTM1	leucine-rich repeats and transmembrane domains 1	-3.84542	0.000157	0.024712
NDST3	N-deacetylase/N-sulfotransferase (heparan glucosaminyl) 3	-3.82115	0.000172	0.025086
ASCL1	achaete-scute complex homolog 1 (Drosophila)	-3.78407	0.000198	0.02575
SARDH	sarcosine dehydrogenase	-3.77114	0.000208	0.025791
DTX3	deltex homolog 3 (Drosophila)	-3.7482	0.000226	0.027
ZNF215	zinc finger protein 215	-3.68747	0.000284	0.030808
KCNK2	potassium channel, subfamily K, member 2	-3.63861	0.00034	0.034696
IGSF3	immunoglobulin superfamily, member 3	-3.63253	0.000348	0.034748
PRLR	prolactin receptor	-3.62432	0.000358	0.034851
GRM4	glutamate receptor, metabotropic 4	-3.62384	0.000359	0.034851
REN	renin	-3.61385	0.000372	0.035074
NPAS1	neuronal PAS domain protein 1	-3.56186	0.000449	0.038932
LY6G6E	lymphocyte antigen 6 complex, locus G6E	-3.51691	0.000528	0.042673
NEBL	nebulette	-3.51145	0.000538	0.042937
GRIN1	glutamate receptor, ionotropic, N-methyl D-aspartate 1	-3.50008	0.000561	0.043839
BMP5	bone morphogenetic protein 5	-3.49547	0.00057	0.043992
ADRA1A	adrenergic, alpha-1A-, receptor	-3.44328	0.000685	0.047783
GFI1B	growth factor independent 1B transcription repressor	-3.41696	0.000751	0.0514
SLC6A11	solute carrier family 6 (neurotransmitter transporter, GABA), member	-3.4121	0.000764	0.051702

	11			
CYP3A43	cytochrome P450, family 3, subfamily A, polypeptide 43	-3.39242	0.000818	0.052859
DTX2	deltex homolog 2 (Drosophila)	-3.37829	0.000859	0.053905
GEMIN7	gem (nuclear organelle) associated protein 7	-3.36442	0.000902	0.055679
DCC	deleted in colorectal carcinoma	-3.35303	0.000938	0.05646
TYR	tyrosinase-like (pseudogene); tyrosinase (oculocutaneous albinism IA)	-3.34637	0.000959	0.057278
PCP4	Purkinje cell protein 4	-3.32926	0.001017	0.059746
CLEC10A	C-type lectin domain family 10, member A	-3.2873	0.001174	0.064009
EDN2	endothelin 2	-3.26893	0.001249	0.066244
LDB3	LIM domain binding 3	-3.26435	0.001268	0.066785
PPY	pancreatic polypeptide	-3.26022	0.001286	0.066808
LOC90925	hypothetical protein LOC90925	-3.25545	0.001307	0.066808
DOK4	docking protein 4	-3.25482	0.001309	0.066808
CEMP1	cementum protein 1	-3.2488	0.001336	0.066808
RREB1	ras responsive element binding protein 1	-3.22775	0.001434	0.069063
ATOH1	atonal homolog 1 (Drosophila)	-3.21949	0.001474	0.069874
TNNI1	troponin I type 1 (skeletal, slow)	-3.1982	0.001582	0.072706
GPR45	G protein-coupled receptor 45	-3.1958	0.001595	0.073008
ANXA9	annexin A9	-3.19128	0.001619	0.07383
KISS1	KiSS-1 metastasis-suppressor	-3.18816	0.001635	0.074314
TSKS	testis-specific serine kinase substrate	-3.17906	0.001685	0.075726
KCNQ2	potassium voltage-gated channel, KQT-like subfamily, member 2	-3.1607	0.00179	0.078683
FLJ20184	hypothetical protein FLJ20184	-3.15415	0.001829	0.079906
USH1C	Usher syndrome 1C (autosomal recessive, severe)	-3.15268	0.001838	0.079906
TNFRSF10C	tumor necrosis factor receptor superfamily, member 10c, decoy without an intracellular domain	-3.14483	0.001886	0.08082
RBP3	retinol binding protein 3, interstitial	-3.13642	0.001939	0.081536
APOBEC1	apolipoprotein B mRNA editing enzyme, catalytic polypeptide 1	-3.12	0.002045	0.083414
AKAP6	A kinase (PRKA) anchor protein 6	-3.11712	0.002064	0.083414

CRYBB1	crystallin, beta B1	-3.11167	0.002101	0.083414
HCN3	hyperpolarization activated cyclic nucleotide-gated potassium channel 3	-3.09871	0.002191	0.08512
ATP6V1B1	ATPase, H+ transporting, lysosomal 56/58kDa, V1 subunit B1	-3.08989	0.002255	0.086295
A4GNT	alpha-1,4-N-acetylglucosaminyltransferase	-3.08678	0.002277	0.086295
FNDC8	fibronectin type III domain containing 8	-3.08561	0.002286	0.086295
ATP1B4	ATPase, (Na+)/K+ transporting, beta 4 polypeptide	-3.07507	0.002365	0.088035
PENK	proenkephalin	-3.0679	0.00242	0.088848
NAP1L4	nucleosome assembly protein 1-like 4	-3.06204	0.002466	0.089228
CDH19	cadherin 19, type 2	-3.04891	0.002572	0.091356
ACTN3	actinin, alpha 3	-3.03098	0.002723	0.092698
ANG	angiogenin, ribonuclease, RNase A family, 5	-3.02569	0.002769	0.093808
PCDHGA3	protocadherin gamma subfamily A, 3	-3.02294	0.002793	0.094227
HRC	histidine rich calcium binding protein	-3.01732	0.002844	0.095123
OR5I1	olfactory receptor, family 5, subfamily I, member 1	-2.99049	0.003095	0.097572
PADI4	peptidyl arginine deiminase, type IV	-2.98878	0.003112	0.097607
B3GALT1	UDP-Gal:betaGlcNAc beta 1,3-galactosyltransferase, polypeptide 1	-2.98477	0.003151	0.097932

Supplemental Table 2. Genes Up-regulated when Comparing Ovarian Tumors from Normal Weight (BMI < 25) versus Overweight/Obese (BMI ≥ 25) Women.

Gene Name	David Gene Name	beta	pval	qval
ITFG1	integrin alpha FG-GAP repeat containing 1	2.975429	0.003245	0.098434
ICMT	isoprenylcysteine carboxyl methyltransferase	2.975799	0.003241	0.098434
SRPR	signal recognition particle receptor (docking protein)	2.976675	0.003233	0.098434
CXCL13	chemokine (C-X-C motif) ligand 13	2.980288	0.003196	0.097932
TTC35	tetratricopeptide repeat domain 35	2.980512	0.003194	0.097932
ERGIC2	ERGIC and golgi 2	2.981139	0.003188	0.097932
BBS4	Bardet-Biedl syndrome 4	2.981241	0.003187	0.097932
MARF5	membrane-associated ring finger (C3HC4) 5	2.981251	0.003186	0.097932
MS4A4A	membrane-spanning 4-domains, subfamily A, member 4	2.982922	0.00317	0.097932
NFIL3	nuclear factor, interleukin 3 regulated	2.985834	0.003141	0.097932
BCAS2	breast carcinoma amplified sequence 2	2.988719	0.003113	0.097607
BIN2	bridging integrator 2	2.991432	0.003086	0.097539
HLA-DMA	major histocompatibility complex, class II, DM alpha	2.99241	0.003077	0.097495
STX12	syntaxin 12	2.992448	0.003076	0.097495
MPHOSPH9	M-phase phosphoprotein 9	2.993968	0.003062	0.097495
POSTN	periostin, osteoblast specific factor	2.994647	0.003055	0.097495
DYRK3	dual-specificity tyrosine-(Y)-phosphorylation regulated kinase 3	2.994974	0.003052	0.097495
NME6	non-metastatic cells 6, protein expressed in (nucleoside-diphosphate kinase)	2.995291	0.003049	0.097495
COPS3	COP9 constitutive photomorphogenic homolog subunit 3 (Arabidopsis)	2.997299	0.00303	0.097495
SNX13	sorting nexin 13	2.999238	0.003011	0.09721

TUSC2	tumor suppressor candidate 2	3.002712	0.002978	0.096668
RGS5	regulator of G-protein signaling 5	3.002867	0.002977	0.096668
ZMAT3	zinc finger, matrin type 3	3.003224	0.002973	0.096668
HLA-DRB1	major histocompatibility complex, class II, DR beta 4; major histocompatibility complex, class II, DR beta 1	3.005869	0.002949	0.096668
CUL2	cullin 2	3.008667	0.002923	0.096198
CTSS	cathepsin S	3.011933	0.002893	0.09596
UMPS	uridine monophosphate synthetase	3.014414	0.00287	0.095578
FAHD2A	fumarylacetoacetate hydrolase domain containing 2A	3.017367	0.002843	0.095123
SAMM50	sorting and assembly machinery component 50 homolog (S. cerevisiae)	3.034131	0.002696	0.092227
PSMB9	proteasome (prosome, macropain) subunit, beta type, 9 (large multifunctional peptidase 2)	3.034322	0.002694	0.092227
CHEK2	protein kinase CHK2-like; CHK2 checkpoint homolog (S. pombe); similar to hCG1983233	3.034329	0.002694	0.092227
ZBTB5	zinc finger and BTB domain containing 5	3.038413	0.002659	0.092227
PBLD	phenazine biosynthesis-like protein domain containing	3.038583	0.002658	0.092227
DAB2	disabled homolog 2, mitogen-responsive phosphoprotein (Drosophila)	3.039081	0.002654	0.092227
ISOC1	isochorismatase domain containing 1	3.040811	0.002639	0.092227
ANAPC1	anaphase promoting complex subunit 1; similar to anaphase promoting complex subunit 1	3.041419	0.002634	0.092227
GIMAP6	GTPase, IMAP family	3.044913	0.002605	0.091986

	member 6			
MT1X	metallothionein 1X	3.046247	0.002594	0.091865
LY86	lymphocyte antigen 86	3.05035	0.00256	0.091205
HEG1	HEG homolog 1 (zebrafish)	3.055065	0.002522	0.090487
CTPS	CTP synthase	3.055809	0.002516	0.090487
SDCCAG3	serologically defined colon cancer antigen 3; similar to Serologically defined colon cancer antigen 3	3.061854	0.002467	0.089228
RARRES1	retinoic acid receptor responder (tazarotene induced) 1	3.062645	0.002461	0.089228
TGFBR2	transforming growth factor, beta receptor II (70/80kDa)	3.064944	0.002443	0.089151
SEC16A	SEC16 homolog A (S. cerevisiae)	3.06624	0.002433	0.089051
TXN2	thioredoxin 2	3.072266	0.002386	0.08842
MS4A6A	membrane-spanning 4-domains, subfamily A, member 6A	3.07458	0.002369	0.088035
IFI35	interferon-induced protein 35	3.076162	0.002357	0.088035
RAP1A	RAP1A, member of RAS oncogene family	3.07827	0.002341	0.087809
TBC1D15	TBC1 domain family, member 15	3.085759	0.002285	0.086295
WDR8	WD repeat domain 8	3.086918	0.002276	0.086295
GCC2	GRIP and coiled-coil domain containing 2	3.087191	0.002274	0.086295
ADK	adenosine kinase	3.091248	0.002245	0.086295
TWF2	twinfilin, actin-binding protein, homolog 2 (Drosophila)	3.093722	0.002227	0.086227
SNRPD3	small nuclear ribonucleoprotein D3 polypeptide 18kDa	3.102406	0.002165	0.084655
SELL	selectin L	3.103068	0.002161	0.084655
USP15	ubiquitin specific peptidase 15	3.106605	0.002136	0.084057
SNAP29	synaptosomal-associated protein, 29kDa	3.110996	0.002106	0.083414
COPZ2	coatomer protein complex, subunit zeta 2	3.111006	0.002106	0.083414
GABARAPL2	GABA(A) receptor-associated protein-like 2	3.111733	0.002101	0.083414
GBA	glucosidase, beta; acid	3.111935	0.002099	0.083414

	(includes glucosylceramidase)			
KDELR2	KDEL (Lys-Asp-Glu-Leu) endoplasmic reticulum protein retention receptor 2	3.113233	0.002091	0.083414
PLAUR	plasminogen activator, urokinase receptor	3.113244	0.00209	0.083414
WDR61	WD repeat domain 61	3.115266	0.002077	0.083414
ZC3H7A	zinc finger CCCH-type containing 7A	3.116933	0.002066	0.083414
CLINT1	clathrin interactor 1	3.118625	0.002054	0.083414
PPP2R3C	protein phosphatase 2 (formerly 2A), regulatory subunit B'', gamma	3.119822	0.002046	0.083414
KIF2A	kinesin heavy chain member 2A	3.13211	0.001966	0.08162
WDR5B	WD repeat domain 5B	3.133142	0.001959	0.08162
CD46	CD46 molecule, complement regulatory protein	3.133857	0.001955	0.08162
CCNH	cyclin H	3.135669	0.001943	0.081536
MPHOSPH6	M-phase phosphoprotein 6	3.136632	0.001937	0.081536
SRGN	serglycin	3.137016	0.001935	0.081536
FCER1G	Fc fragment of IgE, high affinity I, receptor for; gamma polypeptide	3.139755	0.001918	0.081536
PDIA6	protein disulfide isomerase family A, member 6	3.143351	0.001895	0.080925
SLC25A44	solute carrier family 25, member 44	3.145965	0.001879	0.080809
TTC4	tetratricopeptide repeat domain 4	3.146457	0.001876	0.080809
QRICH1	glutamine-rich 1	3.149489	0.001857	0.080456
SPSB1	splA/ryanodine receptor domain and SOCS box containing 1	3.153107	0.001835	0.079906
C3AR1	complement component 3a receptor 1	3.161055	0.001788	0.078683
MMACHC	methylmalonic aciduria (cobalamin deficiency) cblC type, with homocystinuria	3.163894	0.001772	0.078433
IL13RA1	interleukin 13 receptor, alpha 1	3.169883	0.001737	0.077473
GIMAP5	GTPase, IMAP family member 5	3.175218	0.001707	0.076406

PLK3	polo-like kinase 3 (Drosophila)	3.18564	0.001649	0.074654
SCAMP3	secretory carrier membrane protein 3	3.201424	0.001565	0.07221
COL1A1	collagen, type I, alpha 1	3.206061	0.001541	0.071656
PELO	pelota homolog (Drosophila)	3.207003	0.001536	0.071656
TMEM186	transmembrane protein 186	3.216482	0.001489	0.070026
LYZ	lysozyme (renal amyloidosis)	3.216871	0.001487	0.070026
ZW10	ZW10, kinetochore associated, homolog (Drosophila)	3.221216	0.001465	0.069747
RRAGC	Ras-related GTP binding C	3.2252	0.001446	0.0691
TNFAIP6	tumor necrosis factor, alpha-induced protein 6	3.225375	0.001445	0.0691
TMEM140	transmembrane protein 140	3.232927	0.001409	0.068236
COQ10B	coenzyme Q10 homolog B (S. cerevisiae)	3.236808	0.001391	0.067816
SLC26A6	solute carrier family 26, member 6; cadherin, EGF LAG seven-pass G-type receptor 3 (flamingo homolog, Drosophila)	3.239502	0.001379	0.06748
TLR2	toll-like receptor 2	3.24267	0.001364	0.067041
ATG4A	ATG4 autophagy related 4 homolog A (S. cerevisiae)	3.243065	0.001362	0.067041
COL5A1	collagen, type V, alpha 1	3.243879	0.001358	0.067041
INTS12	integrator complex subunit 12	3.244605	0.001355	0.067041
SLC25A20	solute carrier family 25 (carnitine/acylcarnitine translocase), member 20	3.248614	0.001337	0.066808
ALAS1	aminolevulinate, delta-, synthase 1	3.251697	0.001323	0.066808
DALRD3	DALR anticodon binding domain containing 3	3.25221	0.001321	0.066808
ARHGDIB	Rho GDP dissociation inhibitor (GDI) beta	3.253291	0.001316	0.066808
SNX10	sorting nexin 10	3.255754	0.001305	0.066808
MAPK1	mitogen-activated	3.256458	0.001302	0.066808

	protein kinase 1			
CYB5R4	cytochrome b5 reductase 4	3.259847	0.001288	0.066808
RAB7A	RAB7A, member RAS oncogene family	3.26971	0.001245	0.066244
KARS	lysyl-tRNA synthetase	3.273871	0.001228	0.065727
LRRC14	leucine rich repeat containing 14	3.279587	0.001205	0.064757
GZMA	granzyme A (granzyme 1, cytotoxic T-lymphocyte-associated serine esterase 3)	3.284155	0.001186	0.06405
PLSCR1	phospholipid scramblase 1	3.284538	0.001185	0.06405
UBAP1	ubiquitin associated protein 1	3.287006	0.001175	0.064009
TOMM22	translocase of outer mitochondrial membrane 22 homolog (yeast)	3.293449	0.001149	0.063198
CCDC109B	coiled-coil domain containing 109B	3.29933	0.001127	0.06264
OSTM1	osteopetrosis associated transmembrane protein 1	3.301385	0.001119	0.06264
PPIE	peptidylprolyl isomerase E (cyclophilin E)	3.304849	0.001106	0.062219
AZI2	5-azacytidine induced 2	3.30582	0.001102	0.062219
MCAM	melanoma cell adhesion molecule	3.311459	0.001081	0.061409
IFRD2	interferon-related developmental regulator 2	3.315881	0.001065	0.060847
LXN	latexin	3.317669	0.001058	0.060847
FBXO38	F-box protein 38	3.32478	0.001033	0.059809
FLAD1	FAD1 flavin adenine dinucleotide synthetase homolog (S. cerevisiae)	3.32523	0.001031	0.059809
MBD4	methyl-CpG binding domain protein 4	3.327913	0.001022	0.059746
WDR70	WD repeat domain 70	3.337961	0.000988	0.058292
SLC33A1	solute carrier family 33 (acetyl-CoA transporter), member 1	3.342665	0.000972	0.057642
CDR2	cerebellar degeneration-related protein 2, 62kDa	3.345947	0.000961	0.057278

STAT1	signal transducer and activator of transcription 1, 91kDa	3.35824	0.000921	0.055764
NAGK	N-acetylglucosamine kinase	3.359838	0.000916	0.055764
EBNA1BP2	EBNA1 binding protein 2	3.361808	0.00091	0.055764
TOMM70A	translocase of outer mitochondrial membrane 70 homolog A (S. cerevisiae)	3.364772	0.000901	0.055679
SH2B3	SH2B adaptor protein 3	3.375746	0.000867	0.054099
CORO1A	coronin, actin binding protein, 1A	3.382152	0.000848	0.053467
BECN1	beclin 1, autophagy related	3.390021	0.000825	0.052859
GAS2L1	growth arrest-specific 2 like 1	3.396433	0.000807	0.052534
AURKAIP1	aurora kinase A interacting protein 1	3.398482	0.000801	0.052444
SDF4	stromal cell derived factor 4	3.40093	0.000795	0.052284
HEMK1	HemK methyltransferase family member 1	3.403689	0.000787	0.052284
THOC5	THO complex 5	3.406858	0.000778	0.05207
LPXN	leupaxin	3.410427	0.000769	0.051714
FASTKD3	FAST kinase domains 3	3.415398	0.000756	0.0514
YTHDF2	YTH domain family, member 2	3.430981	0.000715	0.049514
SF3A1	splicing factor 3a, subunit 1, 120kDa	3.442775	0.000686	0.047783
FAP	fibroblast activation protein, alpha	3.446076	0.000679	0.047783
TMEM110	transmembrane protein 110; musculoskeletal, embryonic nuclear protein 1	3.446145	0.000678	0.047783
LAIR1	leukocyte-associated immunoglobulin-like receptor 1	3.451402	0.000666	0.04763
SDS	serine dehydratase	3.459563	0.000647	0.046943
ZBTB40	zinc finger and BTB domain containing 40	3.464996	0.000635	0.046331
TMEM165	transmembrane protein 165	3.481659	0.000599	0.044217
ATP6V1C1	ATPase, H+ transporting, lysosomal 42kDa, V1	3.482951	0.000596	0.044217

	subunit C1			
NR3C1	nuclear receptor subfamily 3, group C, member 1 (glucocorticoid receptor)	3.487975	0.000585	0.044049
ATP6V0B	ATPase, H+ transporting, lysosomal 21kDa, V0 subunit b	3.489342	0.000582	0.044049
NADK	NAD kinase	3.4899	0.000581	0.044049
MACF1	microtubule-actin crosslinking factor 1	3.490847	0.000579	0.044049
TRIM22	tripartite motif-containing 22	3.496602	0.000568	0.043992
B2M	beta-2-microglobulin	3.504998	0.000551	0.04336
GPR65	G protein-coupled receptor 65	3.505009	0.000551	0.04336
RAB5C	RAB5C, member RAS oncogene family	3.513949	0.000534	0.042839
CCL4	chemokine (C-C motif) ligand 4	3.520718	0.000521	0.042381
ATP6V1A	ATPase, H+ transporting, lysosomal 70kDa, V1 subunit A	3.52506	0.000513	0.042012
SEC22A	SEC22 vesicle trafficking protein homolog A (S. cerevisiae)	3.525591	0.000512	0.042012
VGLL3	vestigial like 3 (Drosophila)	3.5275	0.000508	0.042012
TFRC	transferrin receptor (p90, CD71)	3.533232	0.000498	0.041651
ATP6V0D1	ATPase, H+ transporting, lysosomal 38kDa, V0 subunit d1	3.540388	0.000485	0.04088
TFEC	transcription factor EC	3.547581	0.000473	0.040119
SLC35E1	solute carrier family 35, member E1	3.554921	0.000461	0.03935
SAMHD1	SAM domain and HD domain 1	3.555376	0.00046	0.03935
CTSK	cathepsin K	3.561861	0.000449	0.038932
SLA	Src-like-adaptor	3.573332	0.000431	0.037898
HLA-DRA	major histocompatibility complex, class II, DR alpha	3.57644	0.000426	0.03775
VCAN	versican	3.579722	0.000421	0.03758
RHOA	ras homolog gene family, member A	3.58531	0.000413	0.037381

RAB5A	RAB5A, member RAS oncogene family	3.602813	0.000387	0.03589
LAPTM5	lysosomal multispanning membrane protein 5	3.605426	0.000384	0.035826
DPYD	dihydropyrimidine dehydrogenase	3.613384	0.000373	0.035074
IL10RA	interleukin 10 receptor, alpha	3.620434	0.000363	0.035004
RNF14	ring finger protein 14	3.626553	0.000355	0.034851
ARHGEF6	Rac/Cdc42 guanine nucleotide exchange factor (GEF) 6	3.631343	0.000349	0.034748
GMFG	glia maturation factor, gamma	3.634541	0.000345	0.034748
SOAT1	sterol O-acyltransferase 1	3.638757	0.00034	0.034696
HUS1	HUS1 checkpoint homolog (S. pombe)	3.641383	0.000337	0.034696
IL2RB	interleukin 2 receptor, beta	3.658249	0.000316	0.033414
FARS2	phenylalanyl-tRNA synthetase 2, mitochondrial	3.669773	0.000303	0.032308
NDUFB3	NADH dehydrogenase (ubiquinone) 1 beta subcomplex, 3, 12kDa	3.677487	0.000295	0.031681
LRP8	low density lipoprotein receptor-related protein 8, apolipoprotein e receptor	3.688705	0.000283	0.030808
APOL3	apolipoprotein L, 3	3.698826	0.000272	0.030079
APEH	N-acylaminoacyl-peptide hydrolase	3.700758	0.00027	0.030079
CD74	CD74 molecule, major histocompatibility complex, class II invariant chain	3.70804	0.000263	0.02961
MFSD1	major facilitator superfamily domain containing 1	3.709437	0.000262	0.02961
ABHD5	abhydrolase domain containing 5	3.71473	0.000257	0.029432
HLA-DPB1	major histocompatibility complex, class II, DP beta 1	3.718543	0.000253	0.029296
ELTD1	EGF, latrophilin and seven transmembrane domain containing 1	3.740251	0.000233	0.027544
HERPUD1	homocysteine-	3.750708	0.000224	0.027

	inducible, endoplasmic reticulum stress-inducible, ubiquitin-like domain member 1			
NEK4	NIMA (never in mitosis gene a)-related kinase 4	3.752824	0.000223	0.027
APOL1	apolipoprotein L, 1	3.75321	0.000222	0.027
GTF2E1	general transcription factor IIE, polypeptide 1, alpha 56kDa	3.771876	0.000207	0.025791
LHFPL2	lipoma HMGIC fusion partner-like 2	3.773798	0.000206	0.025791
CD247	CD247 molecule	3.778095	0.000202	0.025791
TFG	TRK-fused gene	3.78272	0.000199	0.02575
NKG7	natural killer cell group 7 sequence	3.785842	0.000197	0.02575
PSME3	proteasome (prosome, macropain) activator subunit 3 (PA28 gamma; Ki)	3.78815	0.000195	0.02575
CD3D	CD3d molecule, delta (CD3-TCR complex)	3.797803	0.000188	0.02575
GIN1	gypsy retrotransposon integrase 1	3.801631	0.000185	0.02575
PSMD7	proteasome (prosome, macropain) 26S subunit, non-ATPase, 7	3.811814	0.000178	0.025233
KPNA1	karyopherin alpha 1 (importin alpha 5)	3.815238	0.000176	0.025204
RAC2	ras-related C3 botulinum toxin substrate 2 (rho family, small GTP binding protein Rac2)	3.81962	0.000173	0.025086
OSTF1	osteoclast stimulating factor 1	3.829957	0.000166	0.024712
AP1G1	adaptor-related protein complex 1, gamma 1 subunit	3.832815	0.000164	0.024712
SLC30A5	solute carrier family 30 (zinc transporter), member 5	3.832914	0.000164	0.024712
SLC31A2	solute carrier family 31 (copper transporters), member 2	3.841574	0.000159	0.024712
FTSJ2	FtsJ homolog 2 (E. coli)	3.842267	0.000159	0.024712
SFT2D2	SFT2 domain containing 2	3.848055	0.000155	0.024712
BGN	biglycan	3.851142	0.000153	0.024712
DHODH	dihydroorotate dehydrogenase	3.853507	0.000152	0.024712

UNC50	unc-50 homolog (C. elegans)	3.870186	0.000142	0.024168
CCL5	chemokine (C-C motif) ligand 5	3.871711	0.000142	0.024168
KLHL18	kelch-like 18 (Drosophila)	3.873486	0.000141	0.024168
CFLAR	CASP8 and FADD-like apoptosis regulator	3.875531	0.00014	0.024168
NAPA	N-ethylmaleimide-sensitive factor attachment protein, alpha	3.877349	0.000139	0.024168
HS3ST3A1	heparan sulfate (glucosamine) 3-O-sulfotransferase 3A1	3.882571	0.000136	0.024168
SNX19	sorting nexin 19	3.890749	0.000132	0.024168
ZDHHC4	zinc finger, DHHC-type containing 4	3.895902	0.000129	0.024168
CCR5	chemokine (C-C motif) receptor 5	3.895965	0.000129	0.024168
RPA3	replication protein A3, 14kDa	3.896686	0.000129	0.024168
TFIP11	tuftelin interacting protein 11	3.899828	0.000127	0.024168
ZNF131	zinc finger protein 131	3.915426	0.00012	0.024015
HLA-DPA1	major histocompatibility complex, class II, DP alpha 1	3.921252	0.000117	0.023876
CD48	CD48 molecule	3.923641	0.000116	0.023876
EWSR1	similar to Ewing sarcoma breakpoint region 1; Ewing sarcoma breakpoint region 1	3.940633	0.000108	0.022918
PLAU	plasminogen activator, urokinase	3.947267	0.000106	0.022732
MFN1	mitofusin 1	3.961498	1.00E-04	0.021893
TREX1	three prime repair exonuclease 1	3.978572	9.35E-05	0.020854
AP1B1	adaptor-related protein complex 1, beta 1 subunit	3.997185	8.69E-05	0.019747
EVI2B	ecotropic viral integration site 2B	4.002707	8.50E-05	0.019694
GIMAP4	GTPase, IMAP family member 4	4.018092	8.00E-05	0.019262
GTF3C3	general transcription factor IIIC, polypeptide 3, 102kDa	4.051625	7.01E-05	0.017948
TXNDC9	thioredoxin domain containing 9	4.05962	6.79E-05	0.017763

TCTA	T-cell leukemia translocation altered gene	4.070506	6.50E-05	0.017385
ADAT1	adenosine deaminase, tRNA-specific 1	4.084569	6.14E-05	0.017198
SNRK	SNF related kinase	4.088061	6.06E-05	0.017198
ATR	ataxia telangiectasia and Rad3 related; similar to ataxia telangiectasia and Rad3 related protein	4.094535	5.90E-05	0.017198
SNAI2	snail homolog 2 (Drosophila)	4.100981	5.75E-05	0.017198
PSMB10	proteasome (prosome, macropain) subunit, beta type, 10	4.104128	5.68E-05	0.017198
GLRX	glutaredoxin (thioltransferase)	4.117738	5.37E-05	0.017198
CEP63	centrosomal protein 63kDa	4.123653	5.25E-05	0.017198
RAB31	RAB31, member RAS oncogene family	4.123728	5.25E-05	0.017198
MYCBP	c-myc binding protein	4.141877	4.87E-05	0.017198
CD53	CD53 molecule	4.153208	4.66E-05	0.017198
APOL6	apolipoprotein L, 6	4.168263	4.38E-05	0.017013
TPST2	tyrosylprotein sulfotransferase 2	4.186272	4.07E-05	0.016335
LIPT1	lipoyltransferase 1	4.211462	3.67E-05	0.015243
CD2	CD2 molecule	4.214681	3.62E-05	0.015243
MRPS30	mitochondrial ribosomal protein S30	4.266927	2.92E-05	0.013025
CYB561D2	cytochrome b-561 domain containing 2	4.291059	2.64E-05	0.012236
ARF4	ADP-ribosylation factor 4	4.293031	2.62E-05	0.012236
CD52	CD52 molecule	4.295198	2.60E-05	0.012236
IFI30	interferon, gamma-inducible protein 30	4.296248	2.59E-05	0.012236
NUP155	nucleoporin 155kDa	4.323515	2.31E-05	0.012236
PRKAA1	protein kinase, AMP-activated, alpha 1 catalytic subunit	4.327062	2.27E-05	0.012236
PTPRC	protein tyrosine phosphatase, receptor type, C	4.354332	2.03E-05	0.012207
ETF1	eukaryotic translation termination factor 1	4.375175	1.86E-05	0.012207
ASCC3	activating signal cointegrator 1 complex subunit 3	4.394201	1.71E-05	0.012207
HCCS	holocytochrome c synthase (cytochrome	4.447838	1.36E-05	0.011155

	c heme-lyase)			
ZBTB11	zinc finger and BTB domain containing 11	4.566012	8.18E-06	0.008959
SPCS1	signal peptidase complex subunit 1 homolog (S. cerevisiae)	4.605288	6.89E-06	0.008299
EIF2B3	eukaryotic translation initiation factor 2B, subunit 3 gamma, 58kDa	4.614382	6.62E-06	0.008299
GMPPB	GDP-mannose pyrophosphorylase B	4.693984	4.66E-06	0.007008
LCP2	lymphocyte cytosolic protein 2 (SH2 domain containing leukocyte protein of 76kDa)	4.742966	3.74E-06	0.006434
GMDS	GDP-mannose 4,6-dehydratase	4.755461	3.54E-06	0.006434
SAMSN1	SAM domain, SH3 domain and nuclear localization signals 1	4.868034	2.12E-06	0.00511
VAMP3	vesicle-associated membrane protein 3 (cellubrevin)	5.101483	7.16E-07	0.002154
ASL	argininosuccinate lyase	5.312724	2.59E-07	0.001041
YIPF5	Yip1 domain family, member 5	5.436012	1.41E-07	0.000851
CASP1	caspase 1, apoptosis-related cysteine peptidase (interleukin 1, beta, convertase)	5.72215	3.34E-08	0.000402

Gynecologic Oncology 133 (2014) 90–97

Contents lists available at ScienceDirect

Gynecologic Oncology

journal homepage: www.elsevier.com/locate/ygyno

Obesity increases tumor aggressiveness in a genetically engineered mouse model of serous ovarian cancer☆

Liza Makowski [a,b,1], Chunxiao Zhou [c], Yan Zhong [c], Pei Fen Kuan [b,d], Cheng Fan [b], Brante P. Sampey [e], Megan Difurio [f], Victoria L. Bae-Jump [b,c,*,2]

[a] Department of Nutrition, University of North Carolina, Chapel Hill, NC, USA
[b] Lineberger Comprehensive Cancer Center, University of North Carolina, Chapel Hill, NC, USA
[c] Division of Gynecologic Oncology, University of North Carolina, Chapel Hill, NC, USA
[d] Department of Biostatistics, University of North Carolina, Chapel Hill, NC, USA
[e] Metabolon, Inc., Durham, NC, USA
[f] Department of Pathology and Laboratory Medicine, University of North Carolina, Chapel Hill, NC, USA

HIGHLIGHTS

- Obesity promotes tumor progression in the KpB mouse model of serous ovarian cancer.
- Gene expression and metabolomic profiling indicated significant differences between ovarian tumors from obese versus non-obese mice, including metabolically relevant pathways.

ARTICLE INFO

Keywords:
Obesity
Ovarian cancer
Mouse model
Metabolomics
Genomics
Biomarkers

ABSTRACT

Objectives. Obesity is associated with increased risk and worse outcomes for ovarian cancer. Thus, we examined the effects of obesity on ovarian cancer progression in a genetically engineered mouse model of serous ovarian cancer.

Methods. We utilized a unique serous ovarian cancer mouse model that specifically deletes the tumor suppressor genes, Brca1 and p53, and inactivates the retinoblastoma (Rb) proteins in adult ovarian surface epithelial cells, via injection of an adenoviral vector expressing Cre (AdCre) into the ovarian bursa cavity of adult female mice (KpB mouse model). KpB mice were subjected to a 60% calories-derived from fat in a high fat diet (HFD) versus 10% calories from fat in a low fat diet (LFD) to mimic diet-induced obesity. Tumors were isolated at 6 months after AdCre injection and evaluated histologically. Untargeted metabolomic and gene expression profiling was performed to assess differences in the ovarian tumors from obese versus non-obese KpB mice.

Results. At sacrifice, mice on the HFD (obese) were twice the weight of mice on the LFD (non-obese) (51 g versus 31 g, $p = 0.0003$). Ovarian tumors were significantly larger in the obese versus non-obese mice (3.7 cm^2 versus 1.2 cm^2, $p = 0.0065$). Gene expression and metabolomic profiling indicated statistically significant differences between the ovarian tumors from the obese versus non-obese mice, including metabolically relevant pathways.

Introduction

Obesity has been linked to increased risk of many cancers, including breast, colon, endometrial, among others [1]. Currently, new cancer cases are in the order of 1.5 million with half a million cancer deaths per year, and nearly one in five are due to obesity [1,2]. It is postulated that hyperglycemia and hyperinsulinemia resulting from overnutrition in obese patients provide abundant nutrients and growth factors to cancer cells, resulting in the ideal environment for tumor initiation and promotion [3]. Chronic inflammation and immunosuppression are also thought to be a link between obesity and cancer [3].

☆ Presented as an oral presentation at the 2013 Annual Meeting of the Society of Gynecologic Oncology in Los Angeles, CA.

* Corresponding author at: University of North Carolina (UNC), Division of Gynecologic Oncology, CB# 7572, Physicians Office Building Rm# B105, Chapel Hill, NC 27599, USA. Fax: +1 919 843 5387.
E-mail address: victoria_baejump@med.unc.edu (V.L. Bae-Jump).

[1] LM was supported by UNC University Cancer Research Fund, NIH AA017376; NIH ES019472; NIH P30DK056350 — Nutrition Obesity Research Consortium (NORC).
[2] VBJ was supported by Gynecologic Cancer Foundation/Florence & Marshall Schwid Ovarian Cancer Research Grant, The North Carolina Translational and Clinical Sciences Institute/NC TraCS $50 K Pilot Grant Program, National Institutes of Health Grant DK056350 to the UNC Nutrition Obesity Research Center, OC110163 Department of Defense/Ovarian Cancer Research Program (DOD/OCRP) Translational Pilot Award.

0090-8258/$ – see front matter © 2013 Elsevier Inc. All rights reserved.
http://dx.doi.org/10.1016/j.ygyno.2013.12.026

Epithelial ovarian cancer (OC) is one of the most deadly cancers with an overall 5-year survival of only 30–40%. Increasing evidence suggests that obesity is a significant risk factor for OC and associated with worse outcomes for this disease [1,4–20]. Given the overall poor prognosis of OC and the rising rate of obesity, it is imperative to investigate obesity as a potential modifiable risk factor that may reverse risk and lead to the prevention and improvement of outcomes for OC. We hypothesize that the metabolic consequences of obesity may play a contributing role in the pathogenesis of OC and may lead to biologically and phenotypically different cancers than those that arise in normal weight women, possibly necessitating distinct treatment strategies. Herein, we assessed the impact of obesity on OC development and progression in a genetically engineered mouse model of serous OC and comprehensively interrogated the obesity-induced carcinogenesis signature through genomic and metabolomic analysis.

Materials and methods

Obesity and the K18-gT$^{+/-}_{121}$;p53$^{fl/fl}$;Brca1$^{fl/fl}$ mouse model

The K18-gT$^{+/-}_{121}$;p53$^{fl/fl}$;Brca1$^{fl/fl}$ (KpB) mouse model (Terry Van Dyke, PhD, NIH) is a unique serous OC mouse model, wherein the tumor suppressor genes, Brca1 and p53 are specifically and somatically deleted and the retinoblastoma (Rb) proteins are inactivated in the adult ovarian surface epithelium [21]. Inactivation of all 3 Rb proteins by T_{121} (a fragment of the SV40 large T antigen) is driven by the keratin 18 (K18) promoter [21]. Expression of the T_{121} transgene and knockout of p53 and Brca1 are conditional and only activated via injection of an adenoviral vector expressing Cre (AdCre) into the ovarian bursa cavity of adult female mice. At approximately 6 months after AdCre injection, tumors develop in the affected ovary, while the un-injected ovary remains normal.

All experimental animals were maintained in accordance with the Institutional Animal Care and Use Committee (IACUC) and the NIH guide for the Care and Use of Laboratory Animals. Recombinant adenovirus Ad5-CMV-Cre (AdCre) was purchased from the University of Iowa Transfer Vector Core at a titer of 10^{11}–10^{12} infectious particles/ml. To maximize weight gain, mice were provided a high-fat diet (HFD, obese group) (60% kcal from fat, Research Diets, New Brunswick, NJ) and control mice (non-obese group) were provided a low-fat diet (LFD) (10% kcal from fat, Research Diets, New Brunswick, NJ) ad libitum, beginning at 6 weeks of age. AdCre injection occurred at 8 weeks to induce OC 6 months later (at 8 months of age) [21]. Thirty-six hours following superovulation, the mice were anesthetized, and a single 1 cm incision was made on the dorsal surface of each mouse. The AdCre was then injected via a needle introduced into the oviduct near the infundibulum and into the ovarian bursa, and the incision was closed. All mice were sacrificed at 8 months of age.

The primary outcome comparison between non-obese and obese mice was the response of tumor growth to the obesity exposure. This was assessed via direct measurement of the tumor at the time of sacrifice. At the time of sacrifice, the ovarian tumors were harvested, wet tumor weights recorded, and tissue was snap frozen in liquid nitrogen for later harvest of mRNA for microarray analysis and metabolites for metabolomic analysis.

Body weight & composition

Prior to starting mice on diet and weekly until sacrifice, body weight was measured. Body composition, including lean mass, fat mass, free water content and total water content, of non-anesthetized mice was also measured at pre- and post-diet exposures using the EchoMRI-100 quantitative magnetic resonance whole body composition analyzer (Echo Medical Systems, Houston, TX).

Blood glucose

Random blood glucose was measured prior to start of diet and at sacrifice using a Bayer Contour Blood Glucose Monitor (Bayer HealthCare LLC, Tarrytown, NY).

mRNA isolation

Approximately 25–50 mg of frozen OC tissue in small fragments was homogenized in RLT lysis buffer. Total RNA was isolated using the RNeasy mini kit and QIAshredder kit (Qiagen Inc., Mississauga, ON) following the manufacturer's instructions. RNA quantity and quality were analyzed by Nanodrop (Thermoscientific, Wilmington, DE).

Gene expression profiling

Microarrays were performed on ovarian tumors from non-obese and obese mice (N = 5/group) using Affymetrix GeneChip Mouse Genome 430 2.0 Arrays. These samples were processed in the Lineberger Comprehensive Cancer Center Genomics Core Facility. The image files were analyzed with GenePix Pro 4.1 and pre-processed via the UNC-Chapel Hill Microarray Database (https://genome.unc.edu) where a Lowess normalization procedure was performed to adjust for Cy3 and Cy5 channel biases [22]. In addition, probes with missing values in 3 or more samples in each of the obese and non-obese groups were removed. Two-class SAM (Significance Analysis of Microarrays, http://www-stat.stanford.edu/~tibs/SAM/) was performed to identify significantly differentially expressed genes using FDR < 0.2. EASE (Expression Analysis Systematic Explorer, http://david.niaid.nih.gov/david/ease.htm) analysis was used to interpret and identify biological themes (gene ontology categories) overrepresented in the gene list obtained from SAM results. The EASE Score was used as statistical measure of overrepresentation of a biological theme. Specifically, the EASE Score is a jackknifed one-tailed Fisher's exact probability which is calculated by removing one gene within the given category from the list and penalizes the statistical significance of categories supported by fewer genes; thus is a more robust measure than the Fisher's exact probability [23].

Metabolomic profiling

Gas chromatography time-of-flight mass spectrometry (GC-TOFMS, Leco Corporation, St Joseph, MI) and liquid chromatography coupled with time-of-flight mass spectrometry (LC-TOFMS, Agilent Corporation, Santa Clara, CA) were used to analyze tumors from non-obese and obese mice (N = 5/group). Metabolite extraction followed previous publication with minor revision through the UNC/Nutrition Obesity Research Center (NORC) Core facility [24]. Briefly, 50 mg samples were extracted with 0.5 ml of methanol:chloroform:water = 3:1:1 (v:v:v) with homogenization for 3 min using 1-mm inner diameter balls in a Bullet Blender (Next Advance, Averill Park, NY). Two aliquots of 150 μl of supernatant were used for GC-TOFMS and LC-TOFMS analysis, separately. After removal of the extra supernatant, the remainder was extracted with 500 μl of methanol. Two aliquots of 150 μl of supernatant were combined into the tube containing first step extraction for GC and LC-TOFMS analysis, separately. Metabolite annotation was performed by comparing the mass spectrum and retention time to an in-house library and NIST library (GC-TOMFS) or HMDB (LC-TOFMS) [25,26].

Statistical methods

Unpaired Student's *t*-test was used to determine statistical difference between non-obese and obese treatment groups using STATA software (College Station, TX). A p-value <0.05 was considered significant. For metabolomics, after normalization to the internal standard and sample weight, the data set was imported into SIMCA-p software

(Umeå, Sweden) for multivariate analysis. Principle component analysis (PCA) was first performed to check the outliers and the separation tendency (data not shown). A supervised orthogonal partial least squares-discriminant analysis (OPLS-DA) analysis was then performed. Differentiating metabolites were selected with the criteria of the variable importance in the projection (VIP) value >1 and p value (Student's *t* test) lower than 0.05.

Results

Obesity drove significant tumor progression in KpB mice

KpB mice were subjected to 60% calories-derived from fat in a high fat diet (HFD) versus 10% calories from fat in a low fat diet (LFD) to induce diet-induced obesity (N = 14/group) starting at 6 weeks of age and until sacrifice. After 8 months of exposure to the HFD or LFD, obese mice weighed significantly greater than non-obese mice ($p = 0.003$, Table 1). There was no effect of HFD on non-fasted blood glucose levels in KpB mice over the course of the diet (Table 1). Body composition was significantly altered in obese KpB mice compared to non-obese controls. Percent body fat was six-fold greater in obese mice (Table 1, $p = 0.0001$), while percent lean mass increased by 25% ($p = 0.0006$, Table 1). The ovarian tumors were tripled in size in the obese mice as compared to non-obese mice (mean size of 3.7 cm^2 versus 1.2 cm^2, Fig. 1, $p = 0.0065$).

Obesity induces genomic differences between obese and non-obese ovarian tumors

439 genes were found to be significantly up-regulated (417 genes) or down-regulated (22 genes) in the ovarian tumors from obese KpB mice versus non-obese mice (FDR < 0.2, Supplemental Table 1). Fig. 2 is a heat map of 131 genes up- and down-regulated at a FDR < 0.1. Metabolically relevant genes were significantly upregulated in the ovarian tumors from the obese versus non-obese mice, such as lipocalin (2.7 fold), fatty acid amide hydrolase (2.7 fold), fatty acid 2-hydroxylase (2.2 fold), glycerol-3-phosphate acyltransferase (1.5 fold), protein phosphatase (1.2 fold), AMP deaminase 3 (1.6 fold), and protein kinase C (1.7 fold) (Supplemental Table 1). Arginase 1 was the most upregulated gene (7.3 fold) and plays a role in the urea cycle, tissue remodeling and inflammation. Other upregulated genes identified in the ovarian tumors from the obese mice were related to cell adhesion, including neurotrimin (2.2 fold) and desmoglein 1-alpha (2.0 fold). Increased expression of histone 1 (2.3 fold), endothelin-1 (5.8 fold), ectonucleoside triphosphate diphosphohydrolase (3 fold) and serotonin transporter solute carrier family 6 member 4 (Slc6a4) (5.4 fold) were also associated with obesity in the KpB mouse model. Significantly downregulated genes with obesity included spermidine synthase and thrombospondin 4.

In the ovarian tumors from the obese versus non-obese mice, EASE over-representation analysis revealed significant enrichment in "phospholipid binding" (EASE score of 0.008), "regulation of apoptosis" (EASE score of 0.014), "lipid binding" (EASE score of 0.015), "endopeptidase activity" (EASE score of 0.03) and "cell–cell signaling" (EASE score of 0.44) for those identified genes.

Table 1
Diet-induced metabolic characteristics in non-obese and obese KpB mice.

	Non-obese	Obese	p-Value
Weight (g)	31.14 ± 5.26	50.71 ± 16.73	p = 0.0003
Glucose (mg/dl)	186.81 ± 26.99	214.38 ± 58.11	p = 0.053
% fat	3.28 ± 1.51	19.58 ± 7.88	p = 0.00001
% lean	22.89 ± 2.11	28.66 ± 5.24	p = 0.0006

N = 14 mice per group. Mean ± SD. % fat or % lean = each mass / total body mass as measured by MRI.

Metabolic differences between ovarian tumors from obese and non-obese KpB mice

Principle component analysis defined a clear separation between obese and non-obese samples (Fig. 3, 3 components, R2X = 0.563, R2Ycum = 0.95, Q2cum = 0.411). Differentiating metabolites were selected with the criteria of the variable importance in the projection (VIP) value >1 and p value (Student's *t* test) lower than 0.05. Twenty metabolites were identified using this criterion, all of which were up-regulated in the ovarian tumors of the non-obese versus obese KpB mice (Table 2).

Metabolites involved in inflammatory signaling and protein/collagen metabolism were down-regulated in the ovarian tumors of obese mice as compared to non-obese mice, including arginine ($p = 0.0268$), N-glycylproline ($p = 0.0043$) and 3-amino-2-piperidone ($p = 0.0099$). Components and markers of oxidative stress were also downregulated in the tumors from obese mice: glutathione ($p = 0.0313$), oxidized glutathione ($p = 0.0047$), gluconolactone ($p = 0.0311$) and 8-hydroxydeoxyguanosine ($p = 0.0230$). Lower levels of nucleotides (i.e. cytidine ($p = 0.0122$ and $p = 0.0424$), cytosine ($p = 0.0158$), guanosine diphosphate (GDP, $p = 0.0404$)) and adenosine monophosphate (AMP, $p = 0.0257$) were detected with obesity. The serotonin metabolite, 5-hydroxyindoleacetic acid (5HIAA, $p = 0.0498$), and the catecholamine metabolites, vanillactic acid ($p = 0.0079$) and phenylethanolamine ($p = 0.0446$), were found to be lower in the ovarian tumors of obese versus non-obese mice. Glutamate ($p = .0318$), N-acetylaspartic acid ($p = 0.0059$) and succinic acid ($p = 0.0465$) are involved in energy metabolism, and were decreased in the ovarian tumors of obese KpB mice. LysoPC(16:1(9Z)) ($p = 0.0205$), a lysophospholipid, was also lower in the ovarian tumors from obese animals.

Discussion

Recent evidence suggests that obesity may be a significant risk factor and associated with worse outcomes for OC [1,4–20]. Therefore, a metabolic approach to the diagnosis and treatment of OC may provide a novel strategy to improve outcomes for this invariably lethal disease. Hence, we induced obesity in the KpB mouse, a faithful murine model of serous OC, to ask if obesity alters tumorigenesis. KpB mice fed a HFD had significant increases in their body weight and fat mass compared to mice fed a LFD. Herein, we report that obesity promoted tumor progression in the KpB mouse model of OC with a tripling of ovarian tumor size. Obesity has been associated with more rapid tumor growth in animal models of other cancer types, such as breast, colon and lung cancer [27,28], but this is the first study to demonstrate this for OC.

Genomic and metabolomic analyses were utilized to identify obesity-induced alterations in tumors with the intention of identifying significant pathways or biomarkers to aid in explaining why obese mice developed larger, more aggressive tumors. The metabolically relevant genes, lipocalin, ectonucleoside triphosphate diphosphohydrolase and fatty acid amide hydrolase, were upregulated in the ovarian tumors from the obese versus non-obese mice. Lipocalin, particularly lipocalin 2, has been previously found to be upregulated in number of different cancers, including OCs [29,30]. The primary function of lipocalin is the transport of small ligands such as steroids, bilins, retinoids and lipids. In addition to its role in lipid transport, lipocalin has also been implicated in the inflammatory response. Another gene significantly upregulated was ectonucleoside triphosphate diphosphohydrolase, which is involved in the extracellular hydrolysis of ATP to generate adenosine, which signals through G-protein coupled receptors and regulates metabolic pathways and inflammation. Chronic inflammation is well known to play a role in obesity-driven cancers which could also explain the increased expression of both lipocalin and ectonucleoside triphosphate diphosphohydrolase in the ovarian tumors of obese KpB mice.

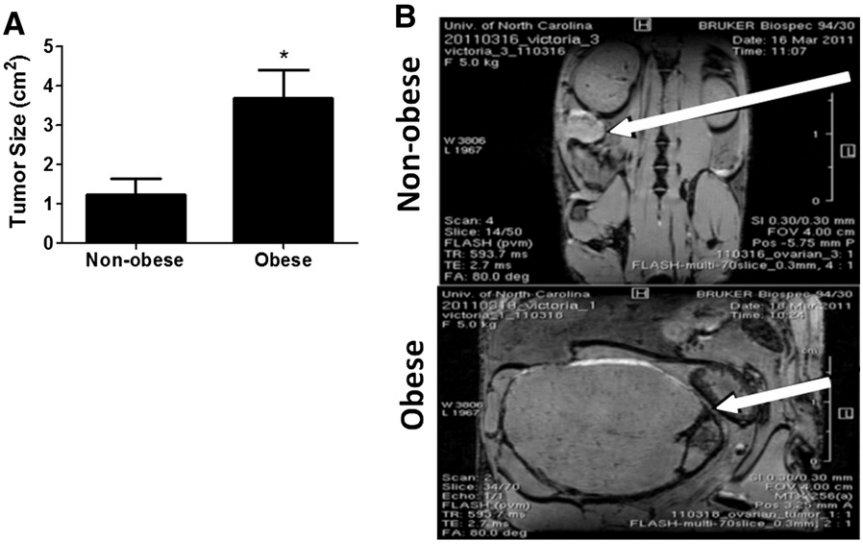

Fig. 1. Obesity increases tumor size in KpB mice. KpB mice were fed low fat or high fat diets to induce obesity for 6 months during tumorigenesis. (A) Comparison of tumor size from non-obese and obese mice (N = 14). These mice were sacrificed 6 months after ovarian tumor induction via injection of AdCre into the ovarian bursa cavity. For the calculation of tumor size, the greatest longitudinal diameter (length) and the greatest transverse diameter (width) were determined and multiplied (m^2). *p = 0.0065. (B) MRI images of tumors (arrow) from non-obese (top image) and obese (bottom image) mice demonstrate representative tumors.

Fatty acid amide hydrolase (FAAH) is a serine hydrolase that metabolizes N-acylethanolamines (i.e. N-arachidonoylethanolamine, N-oleoylethanolamine and N-palmitoylethanolamine), also known as endocannabinoids, to fatty acids plus ethanolamine. The endocannabinoid system is thought to be important in the regulation of cancer cell apoptosis, proliferation, migration, adhesion and invasion. Increased expression of the cannabinoid receptors (CB1R and CB2R) and FAAH has been documented in prostate and breast cancer and has been associated with worse outcomes [31]. FAAH inhibitors are under development for the treatment of pain and inflammation [31], but may also be useful in cancer. Our data suggests that FAAH inhibitors might be a potential targeted agent for obesity-driven cancers.

Other unique, metabolically relevant genes that were associated with obesity and OC development in the KpB mouse model included fatty acid 2-hydroxylase, glycerol-3-phosphate acyltransferase, protein phosphatase, protein kinase C and AMP deaminase. Fatty acid 2-hydroxylase (FA2H) catalyzes the synthesis of 2-hydroxysphingolipids, a subset of sphingolipids that contain 2-hydroxy fatty acids. FA2H is thought to be involved in the cell differentiation of Schwann cells, keratinocytes and adipocytes. Glycerol-3-phosphate acyltransferase is an enzyme that participates in glycerolipid metabolism and glycerophospholipid metabolism. Protein phosphatases are essential to protein phosphorylation, an important form of reversible protein posttranslational modification involved in cell signaling cascades. The protein kinase C (PKC) family represents a number of protein kinase enzymes that are involved in regulating the function of other proteins through the phosphorylation

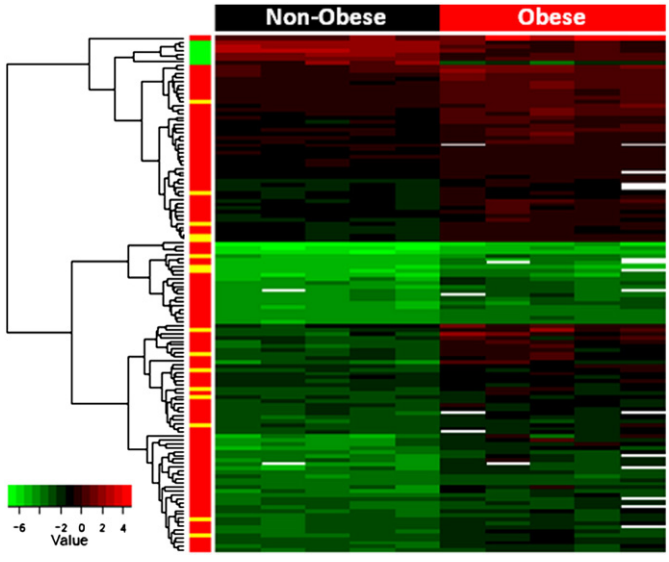

Fig. 2. Genomic differences between ovarian tumors from obese versus non-obese KpB mice reveal alterations in metabolically relevant genes. Heat map representation of 131 genes found to be significantly up- or down-regulated in the ovarian tumors from the obese versus non-obese KpB mice (FDR < 0.1). Many metabolically relevant genes, such as lipocalin, fatty acid amide hydrolase, ectonucleoside triphosphate diphosphohydrolase, fatty acid 2-hydroxylase, glycerol-3-phosphate acyltransferase, protein phosphatase, protein kinase C and AMP deaminase 3, were upregulated in obese tumors.

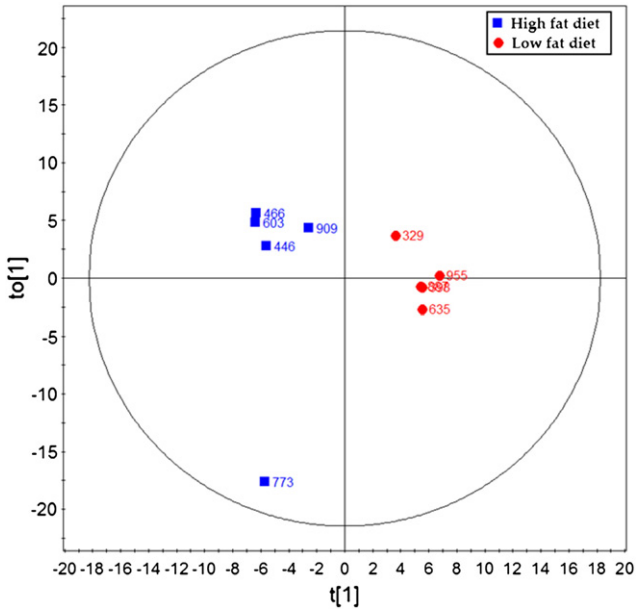

Fig. 3. Several metabolites define a clear separation using principal component analysis between the ovarian tumors in the non-obese group and obese group. PLS-DA scores plot of the ovarian tumors in the non-obese group (low fat diet) and obese (high fat diet) group.

Table 2
Metabolic alterations in tumors from non-obese and obese KpB mice.

Compound name	VIP[a]	p[b]	Fold change (non-obese/obese)[c]	Analysis method	Identification method[d]
N-glycylproline	2.27	0.0043	1.95	LC-ES+	Std
Oxidized glutathione	2.25	0.0047	3.45	LC-ES+	Std
N-acetylaspartic acid	2.22	0.0059	2.31	LC-ES−	HMDB
Vanillactic acid	2.17	0.0079	2.23	LC-ES+	HMDB
3-Amino-2-piperidone	2.14	0.0099	1.75	GCTOF	NIST
Cytidine	2.10	0.0122	4.52	LC-ES+	Std
Cytosine	2.05	0.0158	4.11	LC-ES+	Std
LysoPC(16:1(9Z))	1.99	0.0205	1.83	LC-ES+	HMDB
8-Hydroxy-deoxyguanosine	1.97	0.0230	2.45	LC-ES+	HMDB
Adenosine monophosphate	1.94	0.0257	1.61	LC-ES−	HMDB
Arginine	1.93	0.0268	1.93	LC-ES+	Std
Gluconolactone	1.89	0.0311	2.97	LC-ES+	Std
Glutathione	1.89	0.0313	3.10	LC-ES+	Std
Glutamate	1.89	0.0318	1.52	GCTOF	Std
Guanosine diphosphate	1.82	0.0404	2.39	LC-ES−	HMDB
Cytidine	1.81	0.0424	4.97	GCTOF	NIST
Inodxyl glucuronide	1.80	0.0439	3.05	LC-ES+	HMDB
Phenylethanolamine	1.80	0.0446	1.69	GCTOF	NIST
Succinic acid	1.78	0.0465	1.90	GCTOF	Std
5-Hydroxyindoleacetic acid	1.76	0.0498	1.85	LC-ES+	HMDB

[a] Variable importance in the projection (VIP) was obtained from OPLS-DA with a threshold of 1.0.
[b] p value was calculated from Student's *t* test.
[c] Fold change with a value larger than 1 indicates a relatively higher concentration in tumors from non-obese (low fat diet-fed) KpB mice, while a value less than 1 means a relatively lower concentration as compared to tumors from obese (high fat diet-fed) KpB mice.
[d] The metabolites were identified by in-house library (Std), NIST library (NIST) or HMBD database (HMDB).

of hydroxyl groups of serine and threonine amino acid residues on these proteins. The PKC family of enzymes has been implicated in the regulation of signal transduction, cell proliferation, metabolism and differentiation through its effects on regulation of the cell cycle. PKC inhibitors are already being evaluated in clinical trials for a variety of different cancers, including OC [32]. AMP deaminase 3 is a highly regulated enzyme that catalyzes the hydrolytic deamination of adenosine monophosphate to inosine monophosphate, a branch point in the adenylate catabolic pathway. AMP deaminase 3 is thought to be a potent regulator of energy metabolism in cells. Increased expression of AMP deaminases has been documented in hepatocellular carcinomas [33] but has not been explored in OC.

Although many metabolically relevant genes were found to be associated with obesity-driven cancers in the KpB mouse model, other upregulated genes and pathways were identified. This included genes related to cell adhesion, including neurotrimin and desmoglein 1-alpha. Expression of neurotrimin and desmoglein 1-alpha has not been previously documented in OCs. Increased expression of histone 1 in the ovarian tumors was also associated with obesity in the KpB mice. Histones are the chief protein component of chromatin and are critical for gene regulation. Endothelin-1 (ET-1) is a highly potent vasoconstrictive peptide and was found to be upregulated 5.8 fold in the ovarian tumors from obese mice. Overexpression of ET-1 has been implicated in the epithelial–mesenchymal transition, a mechanism by which transformed epithelial cells acquire the ability to proliferate, invade, resist apoptosis and metastasize [34]. In chemoresistant ovarian cancer cells, ET-1 has been found to be upregulated, leading to enhanced signaling through the MAPK and mTOR/Akt pathway, increased cell proliferation and reduced sensitivity to cisplatin and paclitaxel [35]. Endothelin receptor antagonists are being developed as potential chemotherapeutic agents for cancer [34]. In the ovarian tumors from the obese versus non-obese mice, DAVID functional annotation analysis revealed significant enrichment in “phospholipid binding”, “regulation of apoptosis”, “lipid binding”, “endopeptidase activity” and “cell–cell signaling”. Thus, the increase in aggressiveness, as manifested by a tripling of tumor size, in the obese KpB mice was accompanied by upregulation of genes involved in metabolic, apoptotic and cell signaling pathways.

Metabolic analysis revealed that 20 metabolites were identified as significantly regulated. In general, metabolomic analysis revealed that multiple metabolites contributed to separation of non-obese and obese mice with each metabolite being down-regulated in tumors derived from obese mice. Arginase 1 was the most up-regulated gene in obese tumors, which explains the lower detection of arginine concentrations. Catabolic disease states such as sepsis, injury and cancer cause an increase in arginine utilization, which can exceed normal body production, leading to arginine depletion. Arginase 1 converts L-arginine into L-ornithine and urea. Nitric oxide (NO) synthase and arginase compete for the same substrate (L-arginine); hence high arginase activity will blunt NO production, limiting potential pro-inflammatory responses necessary in tumoricidal immune responses. Indeed, arginase 1 is a marker of the M2, alternatively activated, macrophage that is often associated with more aggressive tumors [36]. Arginase also drives polyamine (such as spermidine) synthesis necessary for proliferation. Spermidine synthase in spermidine synthesis was a down-regulated gene in tumors from obese animals, perhaps in a negative feedback mechanism due to elevated delivery of ornithine generated by arginase 1 (30% lower levels of spermidine were detected in ovarian tumors of obese mice but this did not reach statistical significance). Ornithine can also be converted to the delta-lactam 3-amino-2-piperidine, and this was significantly blunted in tumors from obese mice. Finally, arginase generates ornithine which is used to generate proline (necessary for collagen synthesis) and glutamate/glutamine. Glutamate was found at lower levels suggesting that arginase was directing ornithine production to modulate collagen synthesis in tumors derived from obese mice. AMP and arginine both activate AMP kinase (AMPK) which stimulates substrate metabolism, while arginine can also activate mTOR [37,38]. Decreased concentrations of both AMP and arginine in the ovarian tumors from obese versus non-obese mice may be a reflection of increased turnover of these metabolites in the rapidly growing tumors in the obese mice, and potential regulation of substrate metabolism.

N-glycylproline, which had the highest VIP contributing to separation between non-obese and obese tumors, was significantly lower in obese tumors relative to non-obese tumors in KpB mice (Table 2, $p = 0.0043$). N-glycylproline is an end product of collagen metabolism, but may be recycled into collagen synthesis, and this suggests a potential difference in tissue remodeling between non-obese and obese mice. Overall, Fig. 4 depicts metabolites and genes related to arginine/polyamine/collagen/glutamine metabolism that were decreased in the ovarian tumors from obese mice, suggesting that diet-induced alterations in the stromal components and

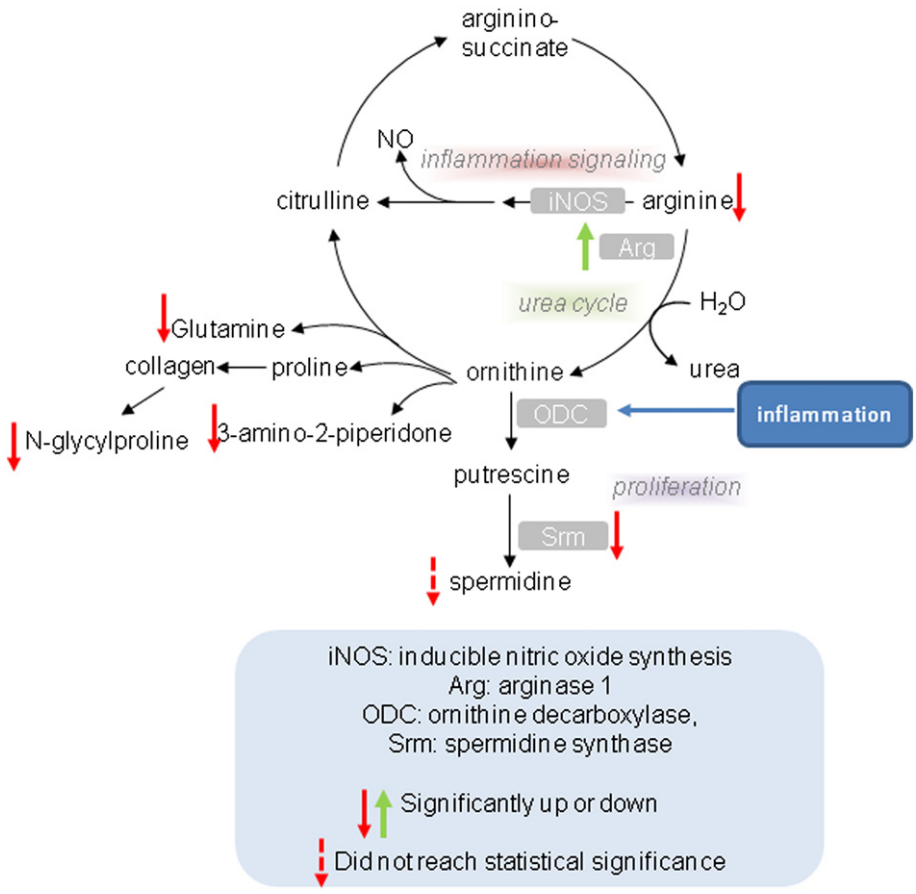

Fig. 4. Obesity-induced alterations in arginine/polyamine/collagen/glutamine metabolism. Metabolomic profiling of ovarian tumors from obese and non-obese KpB mice revealed significant decreases in a number of metabolites related to arginine/polyamine/collagen/glutamine metabolism, suggesting that diet-induced alterations in the stromal components and extracellular matrix are associated with greater growth of the ovarian tumors in obese animals.

extracellular matrix are associated with greater growth of the ovarian tumors in obese animals.

Although glutathione disulfide (GSSG) and glutathione (GSH) were significantly regulated by diet, the ratio of the two (as an indicator of oxidative stress) was not significantly different between lean (0.5 −/+ 0.048) and obese (0.45 −/+ 0.284) tumors, suggesting that there was no active oxidative stress. However, a more stable marker of oxidative stress-induced DNA modification, 8-hydroxydeoxyguanosine, was detected at significantly lower concentrations in obese versus non-obese tumors. Lower concentrations of gluconolactone, an oxidized derivative of glucose, were also found in tumors from obese animals relative to lean, providing further evidence of changes in reduction–oxidation status between the ovarian tumors in the non-obese versus obese group. In sum, in ovarian tumors in obese KpB mice, there appears to be less DNA modification and markers of oxidized metabolites due to oxidative stress, suggesting that oxidative stress is not a major driver of obesity-driven tumorigenesis in the KpB mice or that compensatory mechanisms exist. Alternatively, it could be that the greater growth of ovarian tumors in the obese animals was driven by inflammatory cytokines produced in adipose tissue and distributed to the tumor through the circulation.

Lower concentrations of nucleotides (i.e. cytidine, cytosine, guanosine diphosphate (GDP), adenosine monophosphate (AMP)) may be reflective of increased cell turnover and alterations in utilization and production of these building blocks in the ovarian tumors from obese versus non-obese mice. We postulate that the observed heightened proliferation in the ovarian tumors from the obese versus non-obese mice, as evidenced by a tripling of tumor size, may result in the increased consumption of nucleotides. In the genomic analysis, we also found a 3-fold increase in ectonucleoside triphosphate diphosphohydrolase. This enzyme catalyzes the breakdown of multi-phosphated nucleotides (i.e. ATP, ADP, etc.) and removes free nucleotides and upstream compounds like AMP and GDP, all of which were significantly decreased in the ovarian tumors from the obese mice. In addition, low AMP detected in the ovarian tumors from obese mice suggests possible elevations in anabolic, ATP-burning processes such as lipid synthesis as well as protein, RNA and DNA synthesis.

5-Hydroxyindoleacetic acid (5HIAA) was significantly lower in obese versus non-obese tumors. 5HIAA is a breakdown product of serotonin. Interestingly, the serotonin transporter solute carrier family 6 member 4 (Slc6a4) was upregulated 5.4 fold by obesity. In addition to its function as a neurotransmitter in the central nervous system, increasing evidence suggests that peripheral serotonin may have pro-proliferative and anti-apoptotic effects and act as a mitogen in cancer cells [39,40]; hence, the obesity-mediated regulation of serotonin is of interest.

The catecholamine metabolites, vanillactic acid and phenylethanolamine, were lower in ovarian tumors derived from obese animals. Catecholamines, including epinephrine and norephinephrine, are known to regulate lipolysis [41]. Several studies report that catecholamine responses are blunted in obese versus non-obese individuals at rest and in response to physical activity, suggestive of decreased sympathetic nervous system activity [41]. A decrease in the catecholamine response in the obese mice could lead to reductions in lipolysis and an increase in fat stores that could be advantageous for cancer cell growth.

Succinic acid and glutamate were also significantly decreased by obesity in tumors (Table 2, $p = 0.0465$ and $p = 0.0318$). Succinate is a metabolite of the tricarboxylic acid cycle (TCA) cycle and an electron donor to complex II (Succinate-Q oxidoreductase) in oxidative metabolism. Glutamate is also the metabolic intermediate of glutaminolysis,

which would feed into the TCA cycle upstream of succinic acid at alpha-ketoglutarate. Interestingly, fructose-6-phosphate did not reach statistical significance (non-obese vs. obese ratio 1.62, $p = 0.0684$) but contributed to principle component analysis variance (VIP was 1.67). Fructose 6-phosphate is an important intermediate in glycolysis. Taken together, low AMP, succinate, glutamate, and fructose 6-phosphate suggest that KpB tumors in obese mice have a substantially altered metabolic phenotype compared to tumors that have arisen in non-obese controls. We are currently investigating the role of glycolysis and oxidative metabolism, along with AMPK and mTOR signaling, in ovarian cancers from obese and non-obese patients.

Finally, cytidine is a precursor of cytodinetriphosphate, which is needed to create phosphatidylcholine (PC) and phosphatidylethanolamine. Interestingly, lysoPC(16:1(9Z)) was also downregulated in the ovarian tumors from obese versus non-obese mice. Lysophospholipids (LPLs) can play a role in signaling through G-protein coupled receptors, and are a readily accessible fat source for cancer cells [42]. LPLs are generated via inflammatory-responsive phospholipase A (PLA) activity, suggesting that there may be altered inflammatory signaling between non-obese and obese tumors, which is currently being explored. In our genomic analysis, significant enrichment was found in "phospholipid binding" in the ovarian tumors from the obese mice, potentially corresponding to increased utilization of lysophospholipids in the setting of obesity and depletion of cytidine and lysoPC.

In conclusion, we demonstrate that the obese state can promote tumor progression in the KpB mouse model of serous OC, resulting in genomic and metabolic differences between tumors arising in the obese versus non-obese state. Our work suggests that the metabolic consequences of obesity may be crucial in the pathogenesis of OC, resulting in *biologically distinct* cancers than those that arise in normal weight women. This may have important implications for the treatment of this disease, such that obesity status may be a critical factor in the individualization of management strategies. Further work will be focused on the investigation of the identified obesity-dependent metabolic biomarkers as well as potential novel targets of treatment that may be specific to obesity-driven OCs.

Conflict of interest statement

The authors declare that there are no conflicts of interest.

Appendix A. Supplementary data

Supplementary data to this article can be found online at http://dx.doi.org/10.1016/j.ygyno.2013.12.026.

References

[1] Calle EE, Rodriguez C, Walker-Thurmond K, Thun MJ. Overweight, obesity, and mortality from cancer in a prospectively studied cohort of U.S. adults. N Engl J Med 2003;348(17):1625–38.
[2] Jemal A, Siegel R, Xu J, Ward E. Cancer statistics. CA Cancer J Clin 2010;60(5):277–300.
[3] Khandekar MJ, Cohen P, Spiegelman BM. Molecular mechanisms of cancer development in obesity. Nat Rev Cancer 2011;11(12):886–95 [Epub 2011/11/25].
[4] Delort L, Kwiatkowski F, Chalabi N, Satih S, Bignon YJ, Bernard-Gallon DJ. Central adiposity as a major risk factor of ovarian cancer. Anticancer Res 2009;29(12):5229–34.
[5] Pavelka JC, Brown RS, Karlan BY, Cass I, Leuchter RS, Lagasse LD, et al. Effect of obesity on survival in epithelial ovarian cancer. Cancer 2006;107(7):1520–4.
[6] Olsen CM, Green AC, Whiteman DC, Sadeghi S, Kolahdooz F, Webb PM. Obesity and the risk of epithelial ovarian cancer: a systematic review and meta-analysis. Eur J Cancer 2007;43(4):690–709.
[7] Leitzmann MF, Koebnick C, Danforth KN, Brinton LA, Moore SC, Hollenbeck AR, et al. Body mass index and risk of ovarian cancer. Cancer 2009;115(4):812–22.
[8] Guh DP, Zhang W, Bansback N, Amarsi Z, Birmingham CL, Anis AH. The incidence of co-morbidities related to obesity and overweight: a systematic review and meta-analysis. BMC Public Health 2009;9:88.
[9] Lahmann PH, Cust AE, Friedenreich CM, Schulz M, Lukanova A, Kaaks R, et al. Anthropometric measures and epithelial ovarian cancer risk in the European Prospective Investigation into Cancer and Nutrition. Int J Cancer 2010;126(10):2404–15.
[10] Schouten LJ, Goldbohm RA, van den Brandt PA. Height, weight, weight change, and ovarian cancer risk in the Netherlands cohort study on diet and cancer. Am J Epidemiol 2003;157(5):424–33 [Epub 2003/03/05].
[11] Fairfield KM, Willett WC, Rosner BA, Manson JE, Speizer FE, Hankinson SE. Obesity, weight gain, and ovarian cancer. Obstet Gynecol 2002;100(2):288–96 [Epub 2002/08/02].
[12] Chionh F, Baglietto L, Krishnan K, English DR, MacInnis RJ, Gertig DM, et al. Physical activity, body size and composition, and risk of ovarian cancer. Cancer Causes Control 2010;21(12):2183–94 [Epub 2010/09/10].
[13] Rodriguez C, Calle EE, Fakhrabadi-Shokoohi D, Jacobs EJ, Thun MJ. Body mass index, height, and the risk of ovarian cancer mortality in a prospective cohort of postmenopausal women. Cancer Epidemiol Biomarkers Prev 2002;11(9):822–8 [Epub 2002/09/12].
[14] Lubin F, Chetrit A, Freedman LS, Alfandary E, Fishler Y, Nitzan H, et al. Body mass index at age 18 years and during adult life and ovarian cancer risk. Am J Epidemiol 2003;157(2):113–20 [Epub 2003/01/11].
[15] Engeland A, Tretli S, Bjorge T. Height, body mass index, and ovarian cancer: a follow-up of 1.1 million Norwegian women. J Natl Cancer Inst 2003;95(16):1244–8.
[16] Reeves GK, Pirie K, Beral V, Green J, Spencer E, Bull D. Cancer incidence and mortality in relation to body mass index in the Million Women Study: cohort study. BMJ 2007;335(7630):1134 [Epub 2007/11/08].
[17] Yang HS, Yoon C, Myung SK, Park SM. Effect of obesity on survival of women with epithelial ovarian cancer: a systematic review and meta-analysis of observational studies. Int J Gynecol Cancer 2011;21(9):1525–32 [Epub 2011/11/15].
[18] Protani MM, Nagle CM, Webb PM. Obesity and ovarian cancer survival: a systematic review and meta-analysis. Cancer Prev Res (Phila) 2012;5(7):901–10 [Epub 2012/05/23].
[19] Ovarian cancer and body size: individual participant meta-analysis including 25,157 women with ovarian cancer from 47 epidemiological studies. PLoS Med 2012;9(4):e1001200 [Epub 2012/05/19].
[20] Engeland A, Bjorge T, Selmer RM, Tverdal A. Height and body mass index in relation to total mortality. Epidemiology 2003;14(3):293–9 [Epub 2003/07/16].
[21] Szabova L, Yin C, Bupp S, Guerin TM, Schlomer JJ, Householder DB, et al. Perturbation of Rb, p53, and Brca1 or Brca2 cooperate in inducing metastatic serous epithelial ovarian cancer. Cancer Res 2012;72(16):4141–53 [Epub 2012/05/24].
[22] Yang YH, Dudoit S, Luu P, Lin DM, Peng V, Ngai J, et al. Normalization for cDNA microarray data: a robust composite method addressing single and multiple slide systematic variation. Nucleic Acids Res 2002;30(4):e15 [Epub 2002/02/14].
[23] Hosack DA, Dennis Jr G, Sherman BT, Lane HC, Lempicki RA. Identifying biological themes within lists of genes with EASE. Genome Biol 2003;4(10):R70 [Epub 2003/10/02].
[24] Pan L, Qiu Y, Chen T, Lin J, Chi Y, Su M, et al. An optimized procedure for metabonomic analysis of rat liver tissue using gas chromatography/time-of-flight mass spectrometry. J Pharm Biomed Anal 2010;52(4):589–96 [Epub 2010/02/27].
[25] Qiu Y, Cai G, Su M, Chen T, Zheng X, Xu Y, et al. Serum metabolite profiling of human colorectal cancer using GC-TOFMS and UPLC-QTOFMS. J Proteome Res 2009;8(10):4844–50 [Epub 2009/08/15].
[26] Fordahl S, Cooney P, Qiu Y, Xie G, Jia W, Erikson KM. Waterborne manganese exposure alters plasma, brain, and liver metabolites accompanied by changes in stereotypic behaviors. Neurotoxicol Teratol 2012;34(1):27–36 [Epub 2011/11/08].
[27] Yakar S, Nunez NP, Pennisi P, Brodt P, Sun H, Fallavollita L, et al. Increased tumor growth in mice with diet-induced obesity: impact of ovarian hormones. Endocrinology 2006;147(12):5826–34 [Epub 2006/09/09].
[28] Ford NA, Dunlap SM, Wheatley KE, Hursting SD. Obesity, independent of p53 gene dosage, promotes mammary tumor progression and upregulates the p53 regulator microRNA-504. PLoS One 2013;8(6):e68089 [Epub 2013/07/11].
[29] Cho H, Kim JH. Lipocalin2 expressions correlate significantly with tumor differentiation in epithelial ovarian cancer. J Histochem Cytochem 2009;57(5):513–21 [Epub 2009/02/04].
[30] Santin AD, Zhan F, Bellone S, Palmieri M, Cane S, Bignotti E, et al. Gene expression profiles in primary ovarian serous papillary tumors and normal ovarian epithelium: identification of candidate molecular markers for ovarian cancer diagnosis and therapy. Int J Cancer 2004;112(1):14–25 [Epub 2004/08/12].
[31] Van Dross R, Soliman E, Jha S, Johnson T, Mukhopadhyay S. Receptor-dependent and receptor-independent endocannabinoid signaling: a therapeutic target for regulation of cancer growth. Life Sci 2013;92(8–9):463–6 [Epub 2012/10/17].
[32] Sobhia ME, Grewal BK, Ml SP, Patel J, Kaur A, Haokip T, et al. Protein kinase C inhibitors: a patent review (2008–2009). Expert Opin Ther Pat 2013;23(10):1297–315 [Epub 2013/06/26].
[33] Szydlowska M, Roszkowska A. Expression patterns of AMP-deaminase isozymes in human hepatocellular carcinoma (HCC). Mol Cell Biochem 2008;318(1–2):1–5 [Epub 2008/05/22].
[34] Bagnato A. The endothelin axis as therapeutic target in human malignancies: present and future. Curr Pharm Des 2012;18(19):2720–33 [Epub 2012/03/07].
[35] Bagnato A, Rosano L. Understanding and overcoming chemoresistance in ovarian cancer: emerging role of the endothelin axis. Curr Oncol Rep 2012;19(1):36–8 [Epub 2012/02/14].
[36] Johnson AR, Milner JJ, Makowski L. The inflammation highway: metabolism accelerates inflammatory traffic in obesity. Immunol Rev 2012;249(1):218–38 [Epub 2012/08/15].
[37] Kong X, Tan B, Yin Y, Gao H, Li X, Jaeger LA, et al. L-Arginine stimulates the mTOR signaling pathway and protein synthesis in porcine trophectoderm cells. J Nutr Biochem 2012;23(9):1178–83 [Epub 2011/12/06].
[38] Kim J, Song G, Wu G, Gao H, Johnson GA, Bazer FW. Arginine, leucine, and glutamine stimulate proliferation of porcine trophectoderm cells through the MTOR-RPS6K-

RPS6-EIF4EBP1 signal transduction pathway. Biol Reprod 2013;88(5):113 [Epub 2013/03/15].
[39] Mohammad-Zadeh LF, Moses L, Gwaltney-Brant SM. Serotonin: a review. J Vet Pharmacol Ther 2008;31(3):187–99 [Epub 2008/05/13].
[40] Liang C, Chen W, Zhi X, Ma T, Xia X, Liu H, et al. Serotonin promotes the proliferation of serum-deprived hepatocellular carcinoma cells via upregulation of FOXO3a. Mol Cancer 2013;12:14 [Epub 2013/02/20].
[41] Zouhal H, Lemoine-Morel S, Mathieu ME, Casazza GA, Jabbour G. Catecholamines and obesity: effects of exercise and training. Sports Med 2013;43(7):591–600 [Epub 2013/04/25].
[42] Kamphorst JJ, Cross JR, Fan J, de Stanchina E, Mathew R, White EP, et al. Hypoxic and Ras-transformed cells support growth by scavenging unsaturated fatty acids from lysophospholipids. Proc Natl Acad Sci U S A 2013;110(22):8882–7 [Epub 2013/05/15].